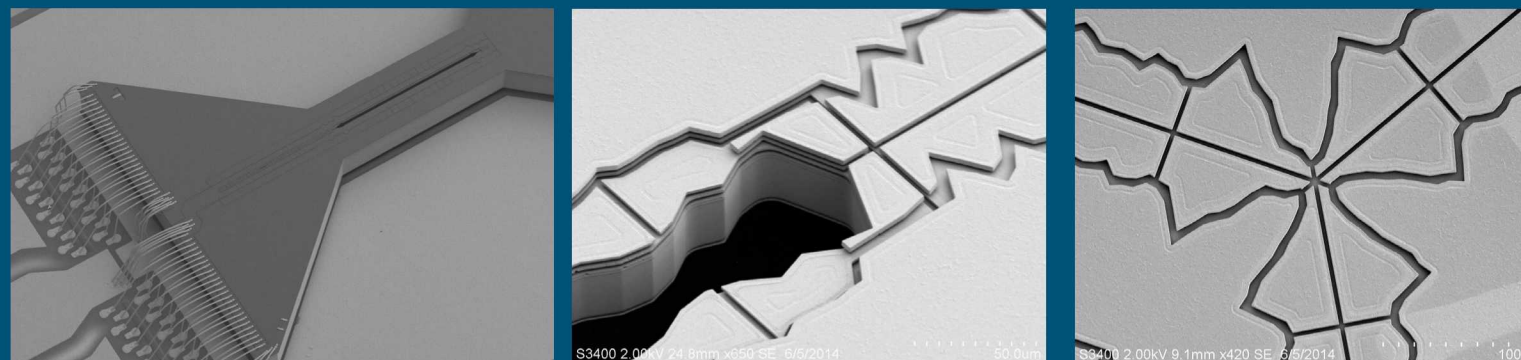
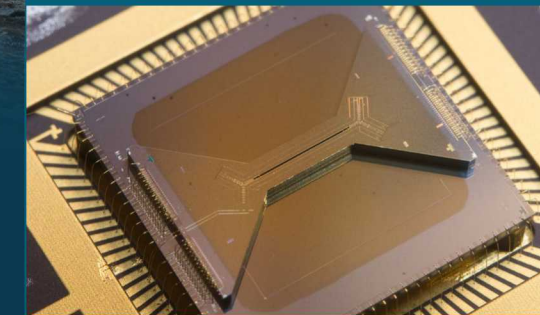


# Science meets Engineering: Design and Realization of the Quantum Scientific Computing Open User Testbed (QSCOUT)



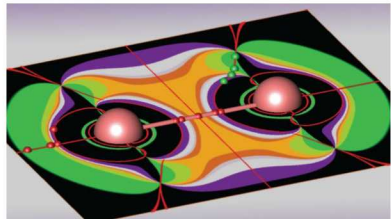
*PRESENTED BY*

Peter Maunz, Sandia National Laboratories



Sandia National Laboratories is a multimission laboratory managed and operated by National Technology & Engineering Solutions of Sandia, LLC, a wholly owned subsidiary of Honeywell International Inc., for the U.S. Department of Energy's National Nuclear Security Administration under contract DE-NA0003525.

# Quantum information



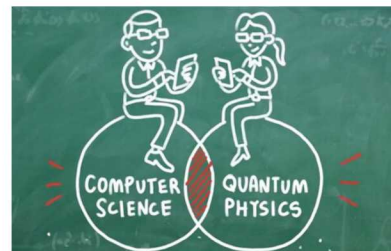
## Quantum chemistry

- Calculation of molecular potentials
- Nitrogen and Oxygen fixation, development of catalytic converters



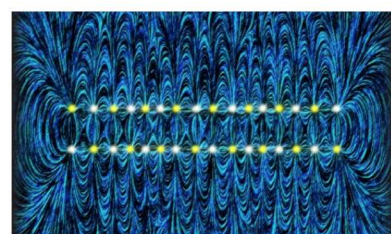
## Medicine

- Structure-based drug development



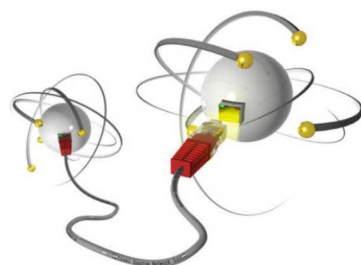
## Quantum computing

- Number factorization (Shor's algorithm)
- Search in unstructured data, searching for solutions to hard problems (Grover's search algorithm)



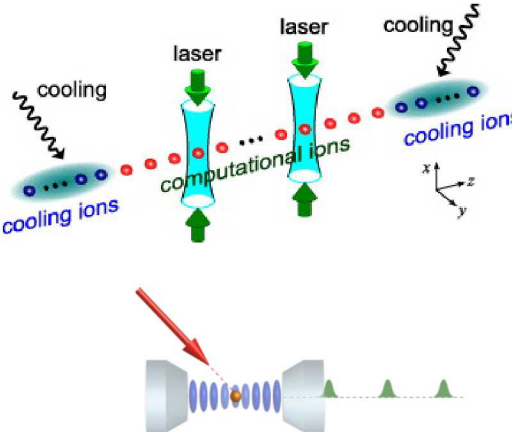
## Quantum simulation

- Simulating many-body systems
- Already for about 20 qubits not possible to simulate classically.



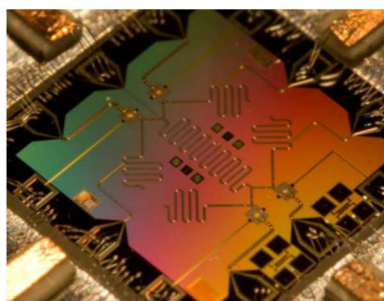
## Quantum Communication

- Securing a quantum channel



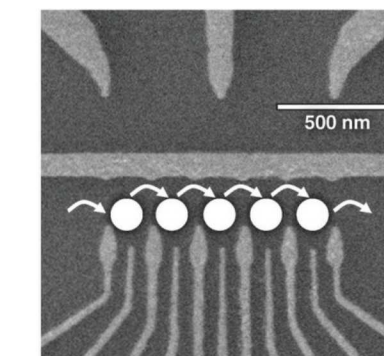
## Trapped Ions

- Blatt and Wineland "Entangled States of Trapped Atomic Ions." *Nature* 453, 1008–15 (2008).
- Monroe and Kim. "Scaling the Ion Trap Quantum Processor." *Science* 339, 1169 (2013)



## Neutral Atoms

- Rydberg states
- Atoms in cavities



## Quantum dots

- Awschalom, et al., "Quantum Spintronics: Engineering and Manipulating Atom-Like Spins in Semiconductors." *Science* 339, 1174 (2013).

### 3 Trapped Ion processors

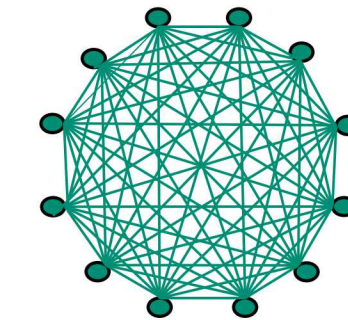
**Best available qubits with history of reliability and quality**

- Ions (qubits) are identical
- Near-ideal prep and measure
  - Error  $< 8 \times 10^{-4}$
- No idle errors (long coherence times)
  - Coherence time  $> 15\text{min}$  possible
- Lowest gate errors
  - Single-qubit error  $< 1 \times 10^{-4}$
  - Two-qubit error  $< 1 \times 10^{-3}$
- Single chain qubit registers demonstrated
- Low crosstalk

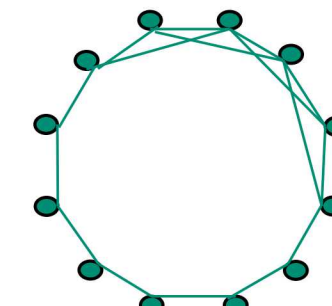
**Reconfigurable in software**

- Optimal for any application
- Change between quantum computer and quantum simulator is change in control
- All-to-All Connectivity
- Ideal for emulating other qubit systems

Trapped Ions:  
fully connected



Solid State:  
2D nearest neighbor  
coupling



## 4 Why microfabrication

- Microfabrication enables scalable traps
  - Junctions and transitions
  - Integration of passive and active components
  - Integration of optics
- Repeatable and reproducible properties
  - Fabrication of identical devices

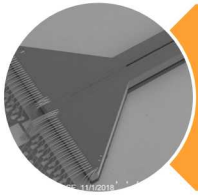


## 5 Challenges of microfabrication

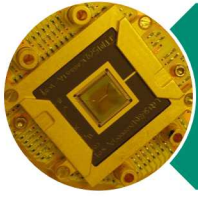
- Microfabrication enables scalable traps
  - Junctions and transitions
  - Integration of passive and active components
  - Integration of optics
- Repeatable and reproducible properties
  - Fabrication of identical devices

- Small distance to electrodes
  - Higher anomalous heating
- Nearby dielectrics
  - Possibly charging of the trap due to scattered laser light
- Small features
  - Sensitive to dust
- Higher anharmonic contributions to trap potential

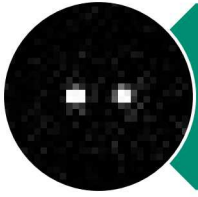
We will demonstrate the state of the art in trap fabrication and demonstrate that microfabricated surface traps can be used for high fidelity quantum operations



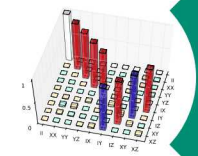
# Trap fabrication capabilities



HOA trap



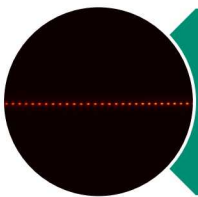
Classical control



Quantum operations



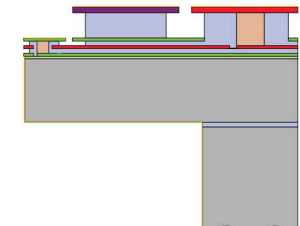
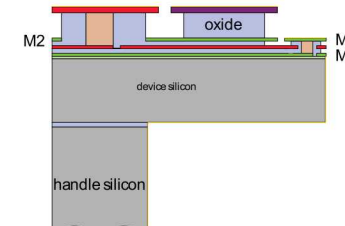
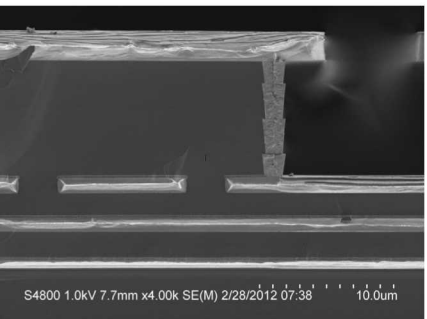
QSCOUT Quantum testbed



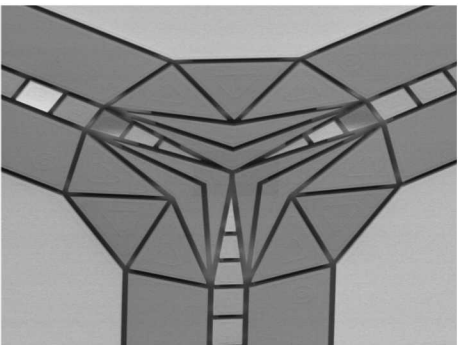
QSCOUT System engineering

## 7 Trap fabrication capabilities

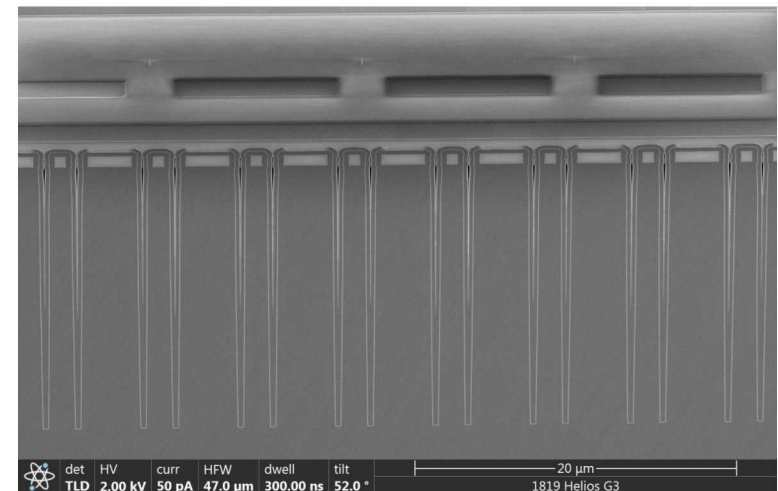
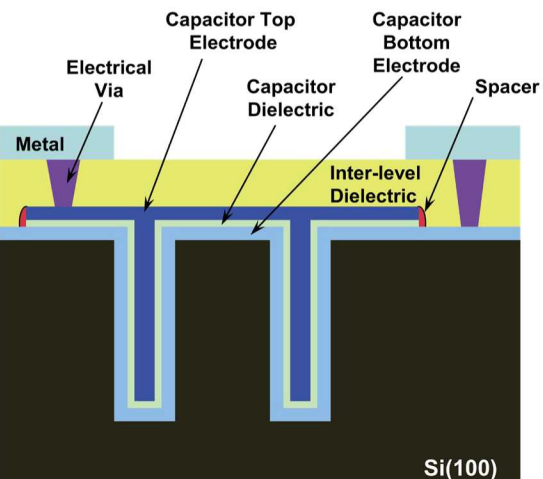
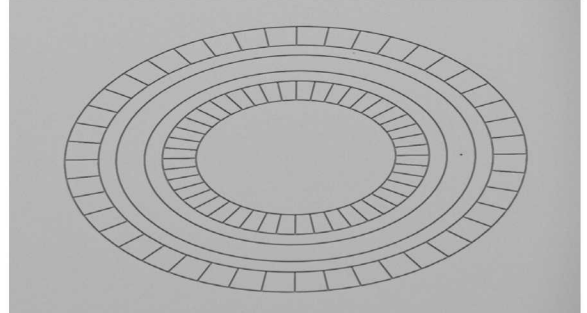
- Based on CEMOS back of line
- Crucial capabilities outside CMOS integrated
- Up to 6-level metallization
  - Planarized
  - Islanded electrodes
  - Reduced rf capacitance
  - Any electrode geometry can be realized
- Removed dielectric (better shielding)
- Integrated trench capacitors for rf shunting
- Loading holes and slots
- Release singulation (e.g. bowtie shapes)



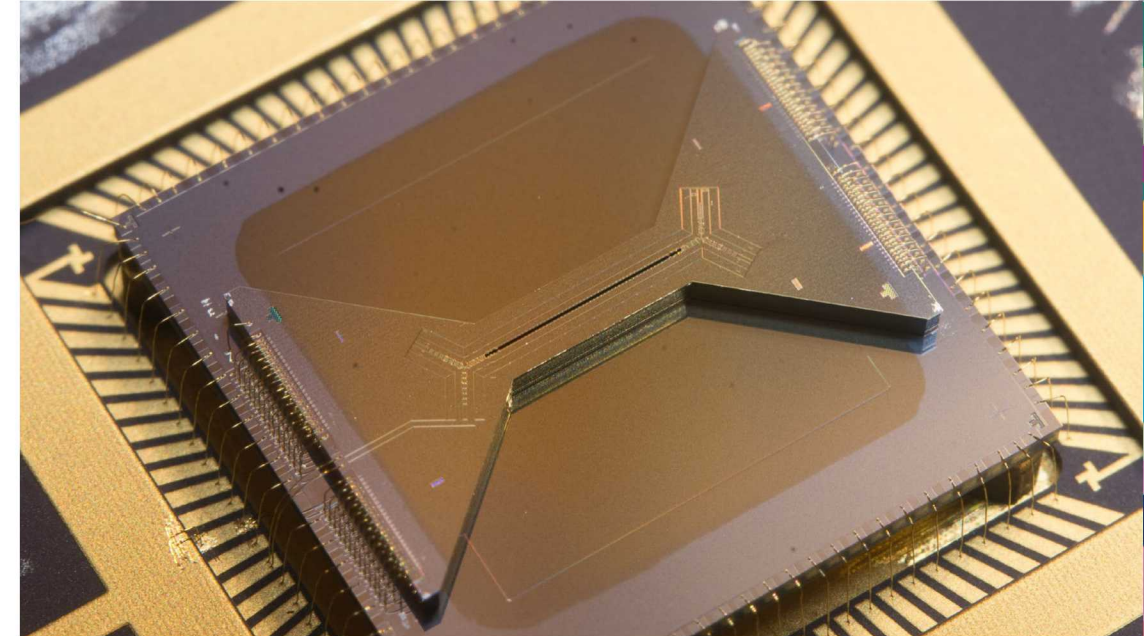
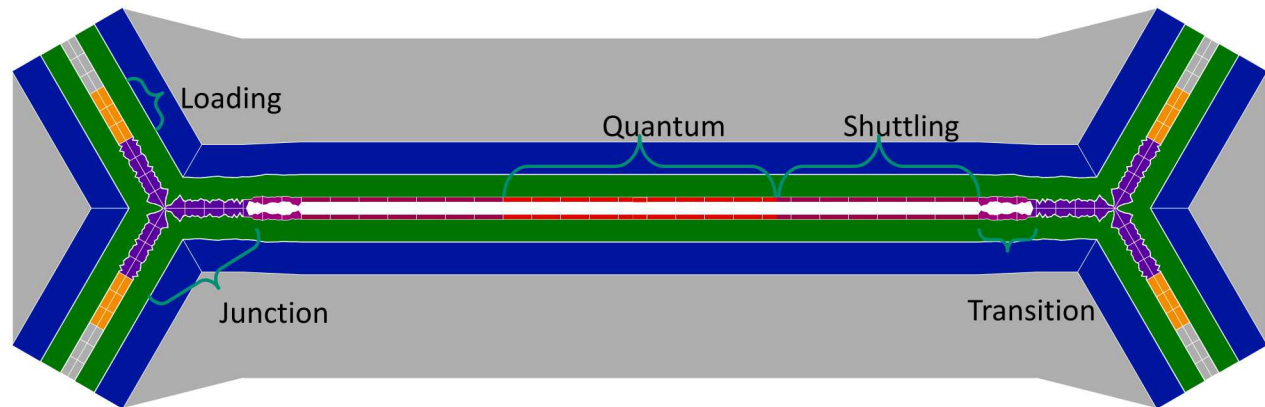
**Switchable Y Junction**



**Ring Trap**



## 8 High Optical Access trap HOA-2



- Excellent optical access rivaling 3-D
  - $2\pi$  for imaging
  - NA=0.2 through slot
  - NA=0.12 skimming surface
- High trap frequencies (characteristic distance 140 $\mu\text{m}$ )
- Full control over principal axes orientation
- Junctions
- Transitions between slotted and above-surface trap regions

## 9 Ytterbium trap characteristics

### Trap frequencies:

- radial 2 - 5 MHz
- rf frequency 50 MHz
- stable for long ion chains

### Heating rates

$$\dot{n}_{\parallel} = 30 \text{ quanta/s}$$

$$\dot{n}_{\perp} \approx 125 \text{ quanta/s}$$

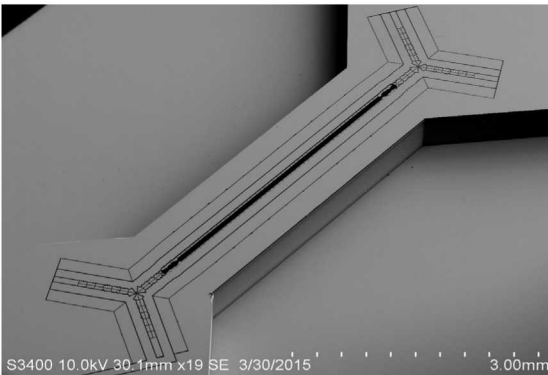
Ytterbium, 2.7 MHz

### Trapping time:

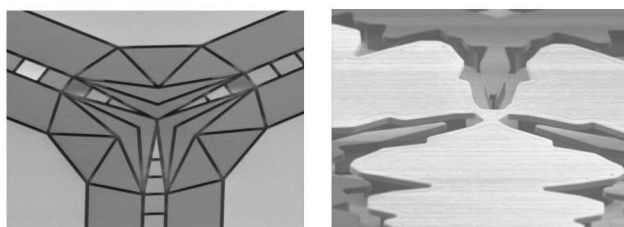
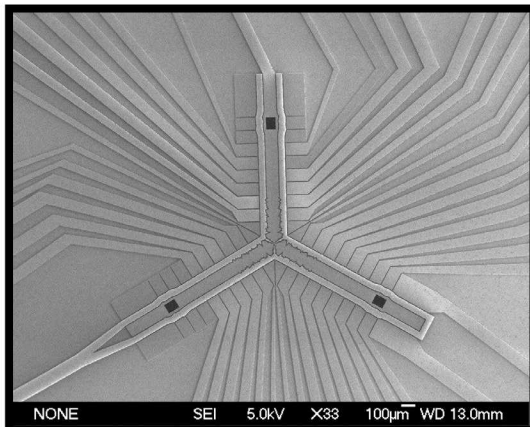
- >100 h observed  
(while running measurements)
- >5 min without cooling

# Some of Sandia's Traps

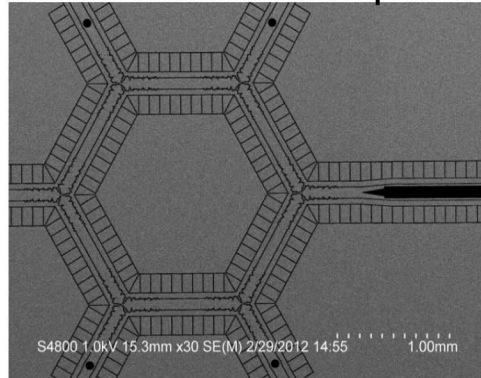
High Optical Access (HOA) trap



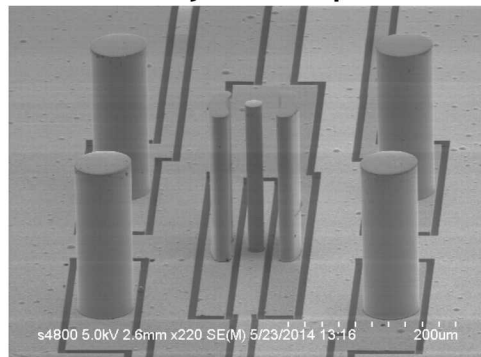
Y-junction traps



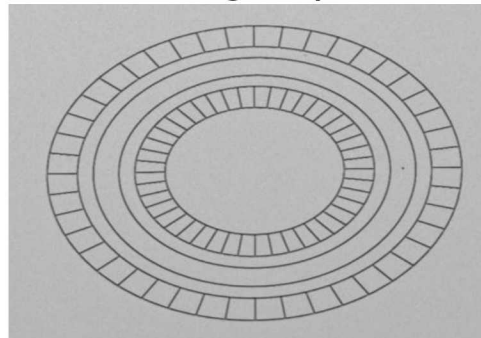
Circulator trap



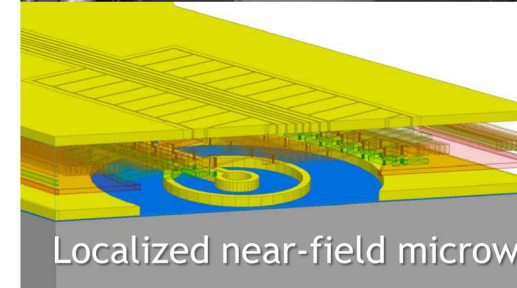
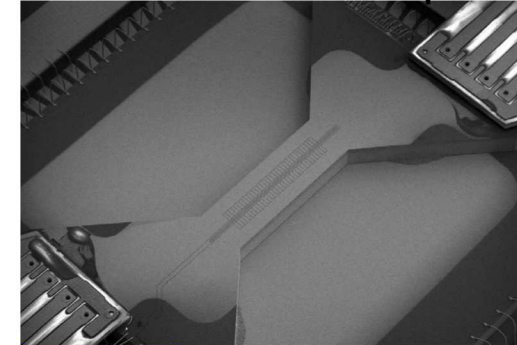
Stylus trap



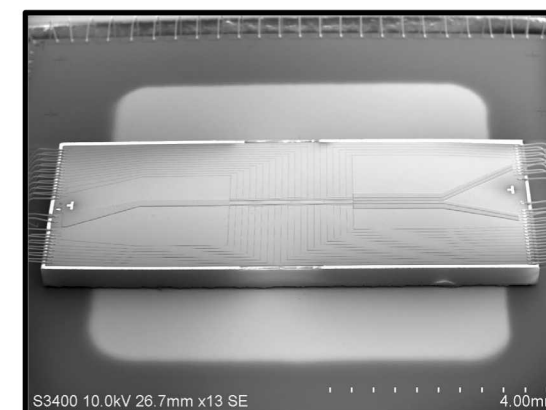
Ring trap



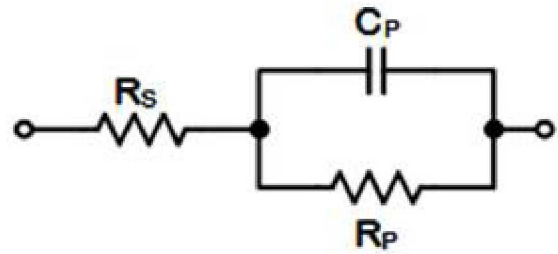
Microwave trap



EPICS trap

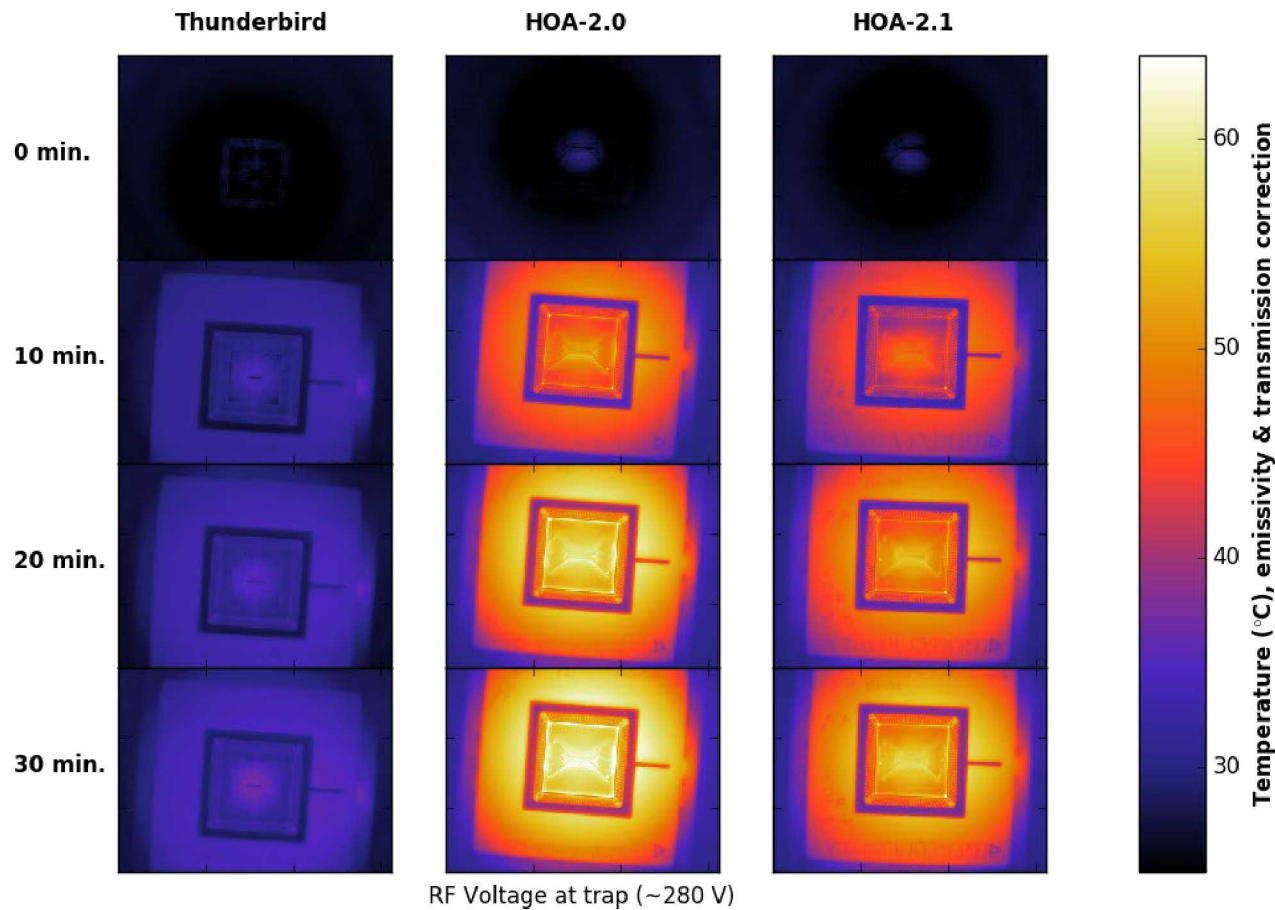


# RF dissipation



$$P_s \approx \frac{1}{2} R_s U^2 \omega^2 C_p^2$$

$$P_p = \frac{1}{2} \frac{\omega U^2}{R_p}$$



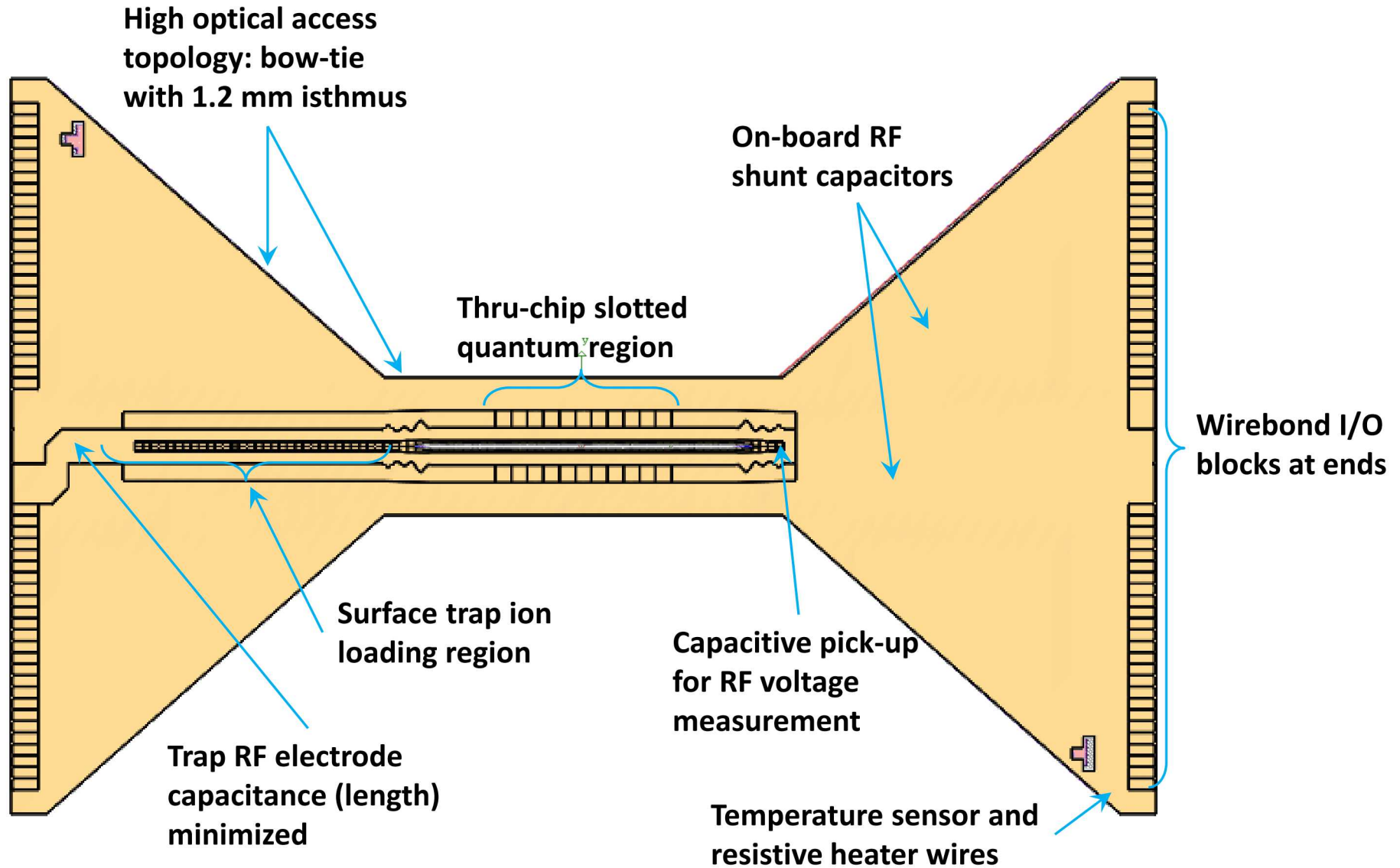
RF Voltage at trap (~280 V)

For 100 V amplitude at 100 MHz:

Trap	Temp	$C_p$	$R_s$	$R_p$	$P_s$	$P_p$
HOA-2	300 K	7.6 pF	1.2 $\Omega$	1.2 M $\Omega$	140 mW	4.2 mW
	4 K		0.5 $\Omega$		60 mW	
HOA-2.1	300 K	7.6 pF	0.9 $\Omega$	1.6 M $\Omega$	100 mW	3.1 mW
	4 K		0.5 $\Omega$		60 mW	
Thunderbird	300 K	2.4 pF	0.6 $\Omega$	1.5 M $\Omega$	6.7 mW	3.3 mW

# Phoenix trap fabrication

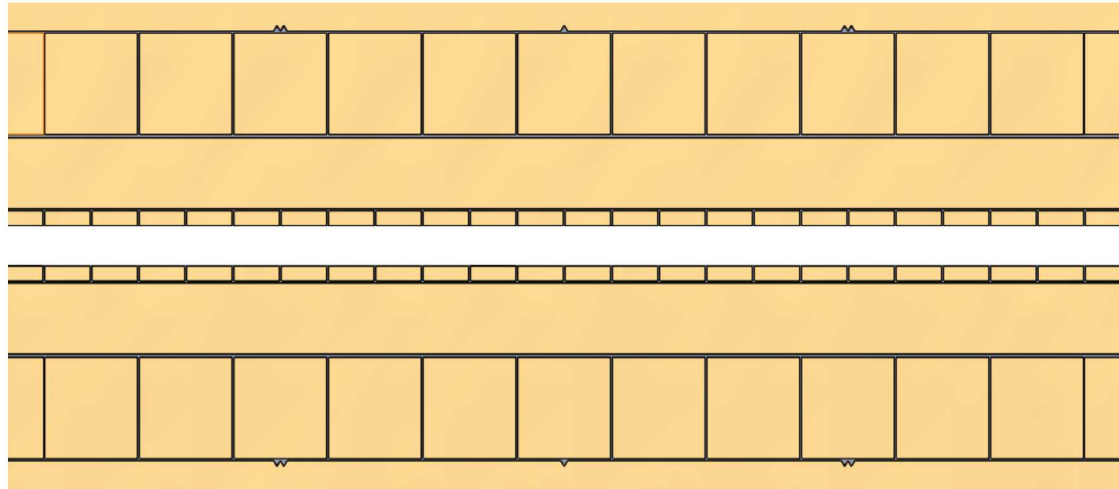
## Original plans for Phoenix



# Phoenix trap fabrication

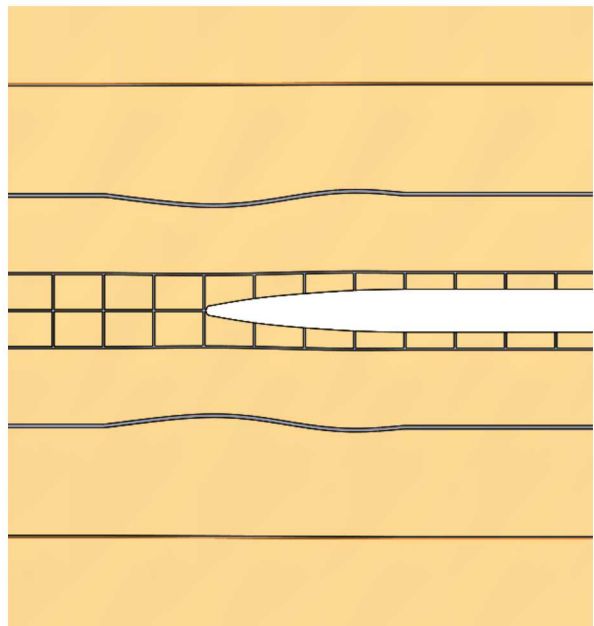
## Trap features

13



### Quantum region

- Segmentation of 22 inner electrode pairs and 11 outer pairs for better control of ion chains and spatial re-ordering of ions
- $22 \times 70 \mu\text{m} = 1540 \mu\text{m}$  long
- Ion height  $70 \mu\text{m}$

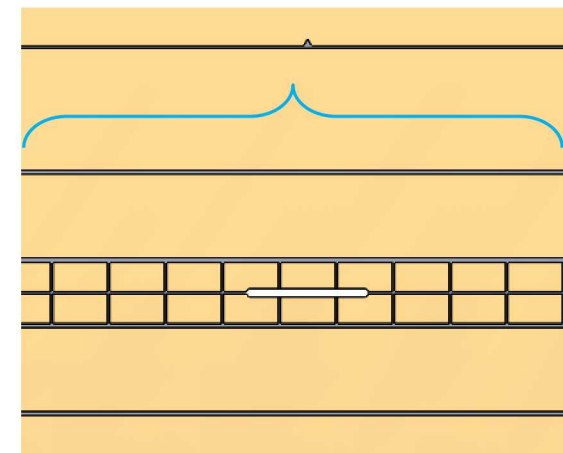


### Transition

- 9 degrees of freedom
- Low spatial frequencies

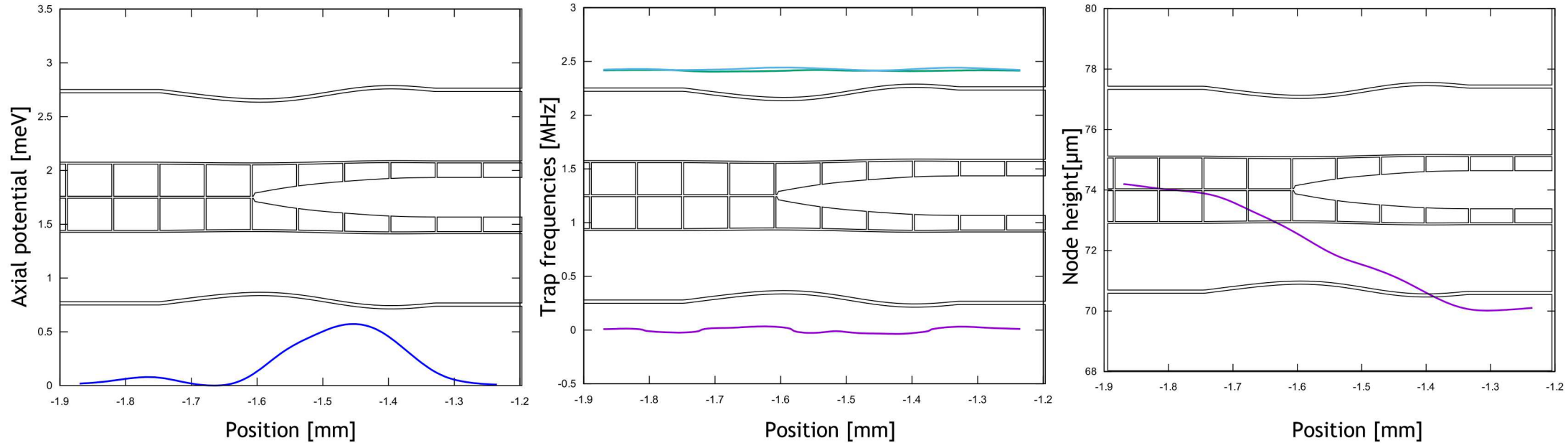
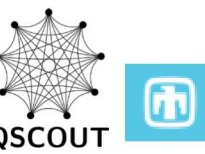
### Loading region

- 5 electrode pairs
- Loading slot  $180 \mu\text{m} \times 3 \mu\text{m}$



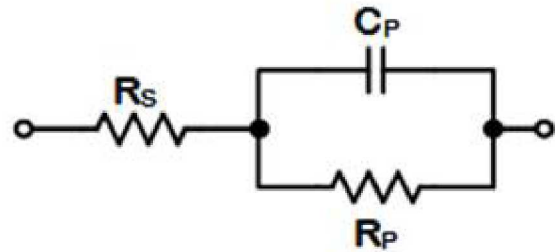
# Phoenix trap Transition characterization

14



- Transition between slotted and above surface parts of trap is optimized to minimize variations in the trace of the curvature tensor
- RF pseudopotential hump is about 0.5meV for a 2.5MHz radial trap frequency
- Ion height above slot and above surface differs to keep trap frequencies (trace of curvature tensor) constant

# Rf-dissipation in traps electrical characterization



$R_s$  : Series resistance (lead resistance)

$R_p$  : (rf) parallel resistance (dielectric absorption)

$C_p$  : capacitance

For 100 V amplitude at 100 MHz:

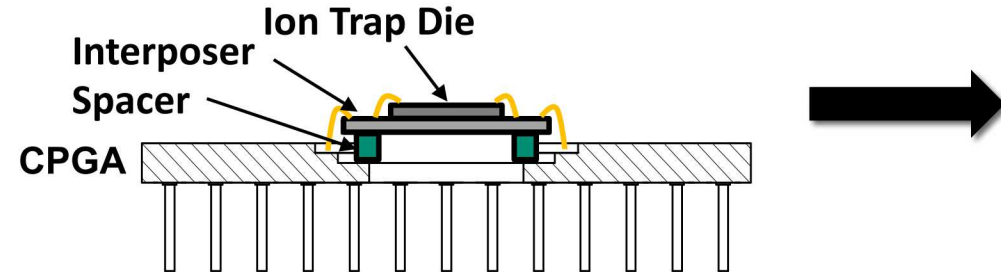
Trap	Temp	$C_p$	$R_s$	$R_p$	$P_s$	$P_p$
Phoenix-0 (measurement)	300 K	4 pF	0.4 $\Omega$		5 mW	
Phoneix-surface (calc.)	4 K		0.05 $\Omega$		1 mW	
Phoenix-slotted (calc.)	300 K	5.5 pF	0.4 $\Omega$		9.4 mW	
	4 K		0.05 $\Omega$		1.4 mW	
HOA-2.1	300 K	7.6 pF	0.9 $\Omega$	1.6 M $\Omega$	100 mW	3.1 mW
	4 K		0.5 $\Omega$		60 mW	
Thunderbird	300 K	2.4 pF	0.6 $\Omega$	1.5 M $\Omega$	6.7 mW	3.3 mW

$$P_s \approx \frac{1}{2} R_s U^2 \omega^2 C_p^2$$

$$P_p = \frac{1}{2} \frac{\omega U^2}{R_p}$$

# Custom trap package

## Legacy 4 Level CPGA Packaging Assembly



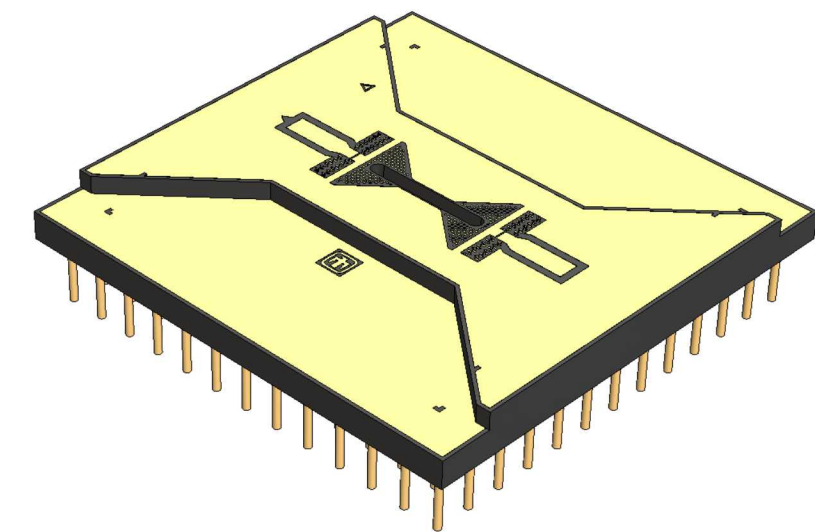
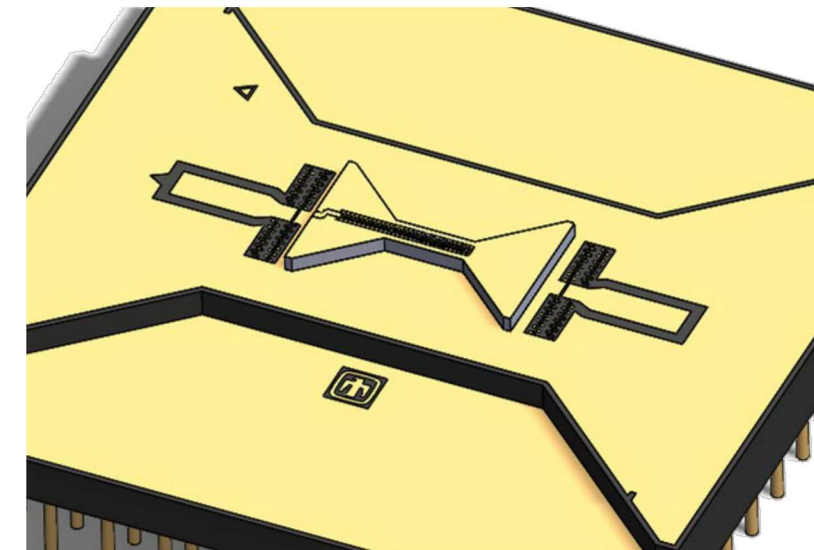
### Objectives:

- Improved rf- and ground performance
- Compatible with bowtie chip without interposer
- Simplified assembly
- Backwards compatibility with MQCO package

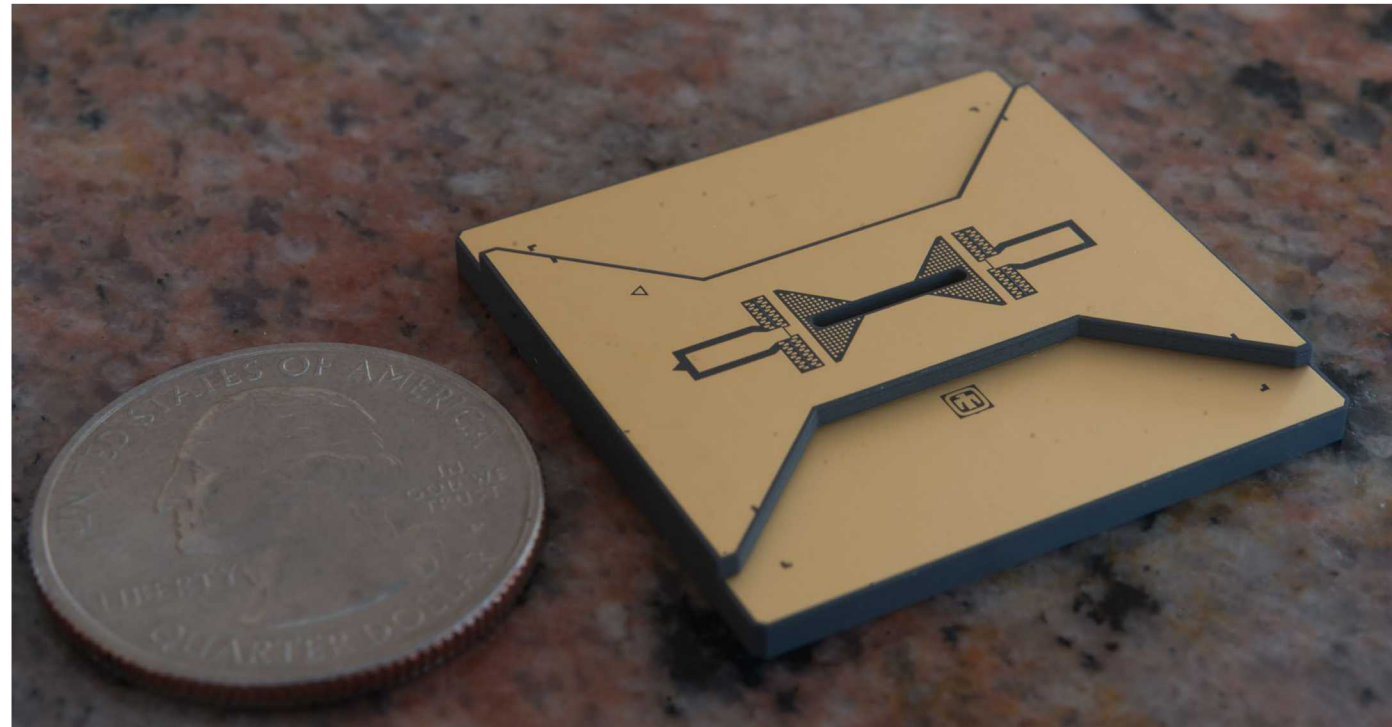
### Properties:

- AlN for improved thermal conductivity and reduced thermal expansion vs  $\text{Al}_2\text{O}_3$
- Two rf connections with minimized capacitance (3pF) and resistivity (50mOhm)
- Backwards compatible with prior HOA devices
- Metal coverage of top surface
- All metal is signal or ground (no floating metals)

## Simplified 2 part assembly

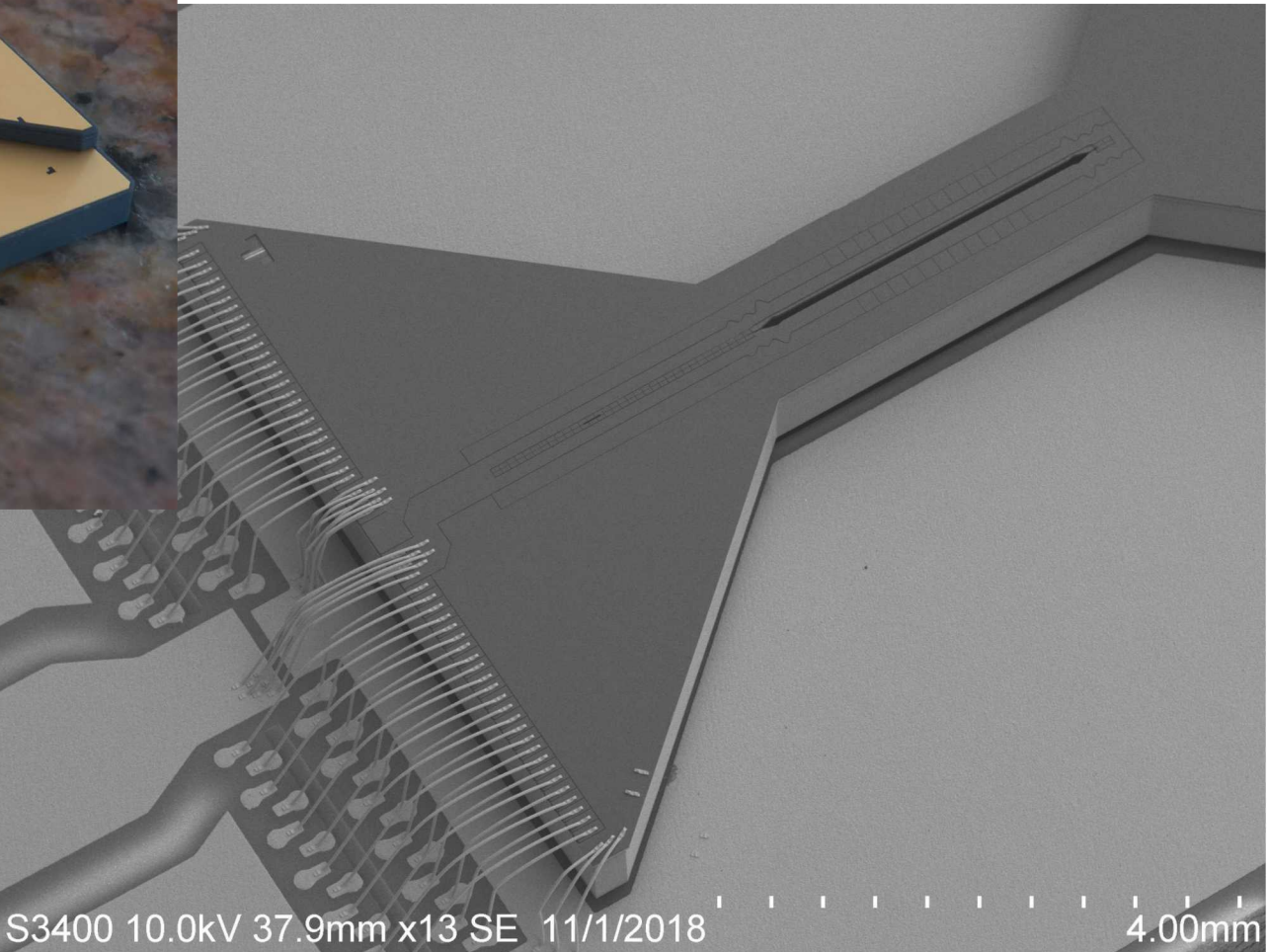


# Custom trap package Is available



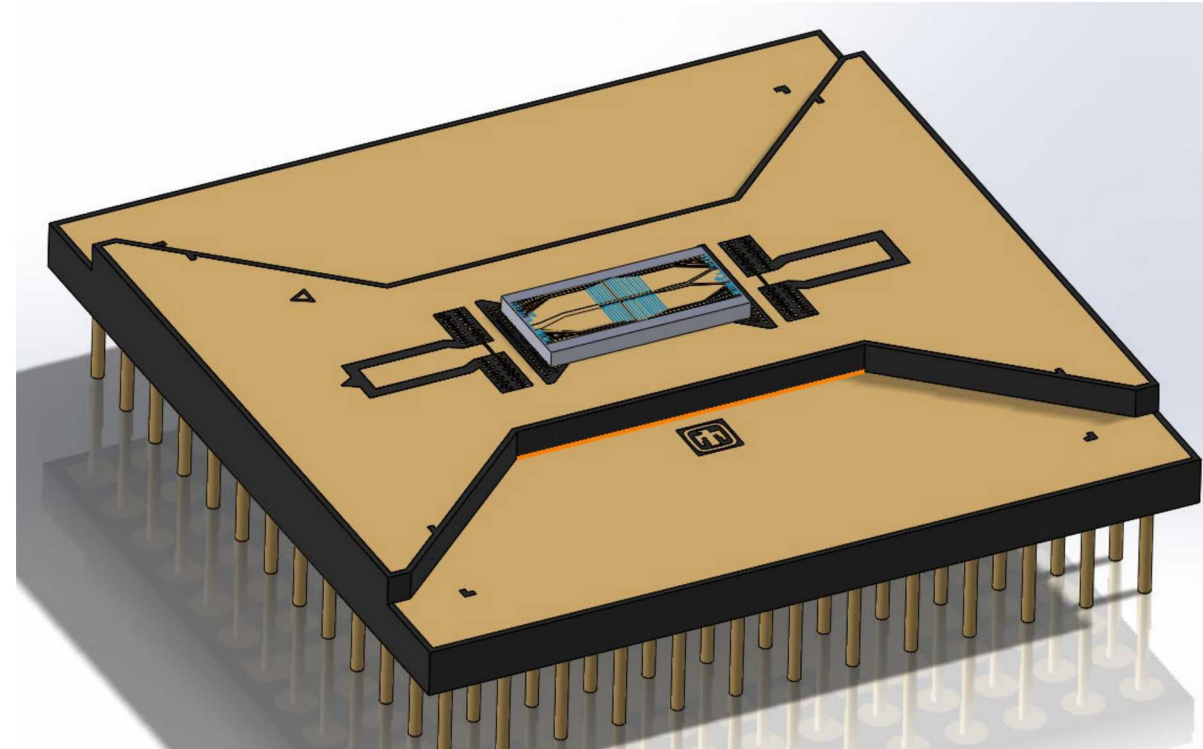
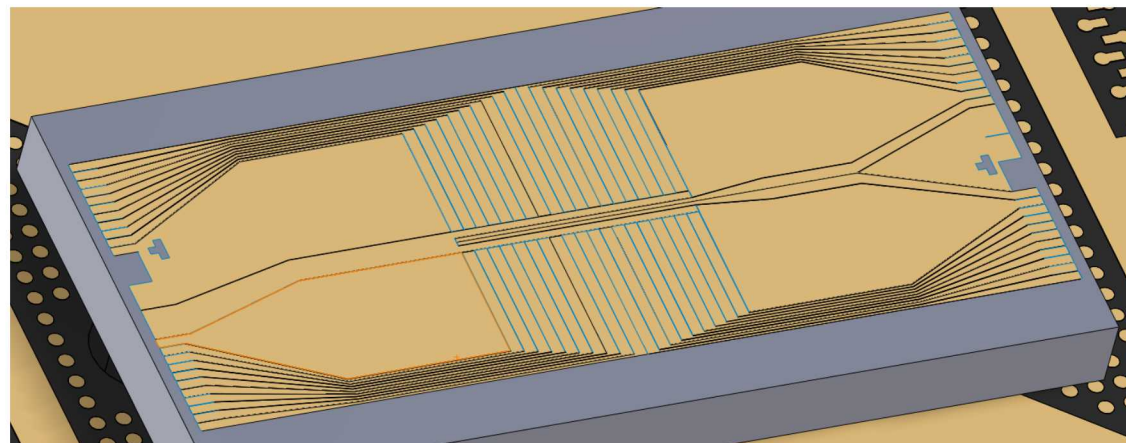
Compared to commercial off the shelf package

- Top surface mostly metal (grounded)
- Low resistance of rf and ground paths  
(massively parallel vias, routing on outer layers)



# Ion heating at cryogenic temperatures

- While ion heating rates at room temperature are good
- Heating rates do not go down as expected when cooling to cryogenic temperatures
- Possible sources of this excess heating
  - **Silicon substrate (ground plane always is the return path for rf currents)**
  - **Vias**
  - **Trench capacitors**
- Scientific approach: investigate influence of silicon substrate
- Use simple single-metal-layer trap on different substrates:
  - Standard silicon  $2\text{-}20\Omega\cdot\text{cm}$
  - High resistivity silicon  $>5\text{k}\Omega\cdot\text{cm}$
  - Float-zone silicon  $>20\text{k}\Omega\cdot\text{cm}$

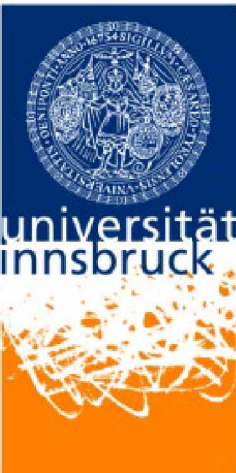




UNIVERSITY OF  
MARYLAND



ETH zürich



Albert-Ludwigs-Universität Freiburg



Georgia  
Tech



Massachusetts  
Institute of  
Technology



JOHANNES GUTENBERG  
UNIVERSITÄT MAINZ



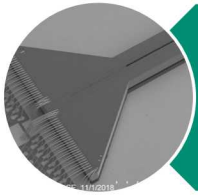
ARL



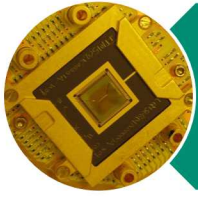
W  
UNIVERSITY of  
WASHINGTON



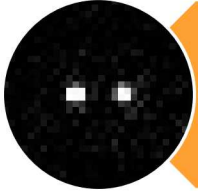
AFRL



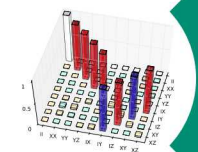
# Trap fabrication capabilities



HOA trap



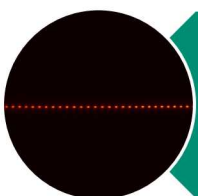
Classical control



Quantum operations



QSCOUT Quantum testbed



QSCOUT System engineering

## Calculating voltage solutions

- Boundary element simulation for surface electrode geometry

$$\mathcal{H} = \begin{pmatrix} \frac{\partial \phi}{\partial x \partial x} & \frac{\partial \phi}{\partial x \partial y} & \frac{\partial \phi}{\partial x \partial z} \\ \frac{\partial \phi}{\partial y \partial x} & \frac{\partial \phi}{\partial y \partial y} & \frac{\partial \phi}{\partial y \partial z} \\ \frac{\partial \phi}{\partial z \partial x} & \frac{\partial \phi}{\partial z \partial y} & \frac{\partial \phi}{\partial z \partial z} \end{pmatrix}$$

- Symmetric curvature tensor
- 6 degrees of freedom
- Determines trap frequencies and principal axes rotations
- Traceless for static fields
- Trace is generated by rf pseudopotential

- Calculate voltage solutions to independently control curvature tensor elements and fields at ion locations
- Use pseudo-inverse to get well-defined solution using nearby electrodes with minimal voltages
- Generate solution for any trap configuration from these basis-solutions

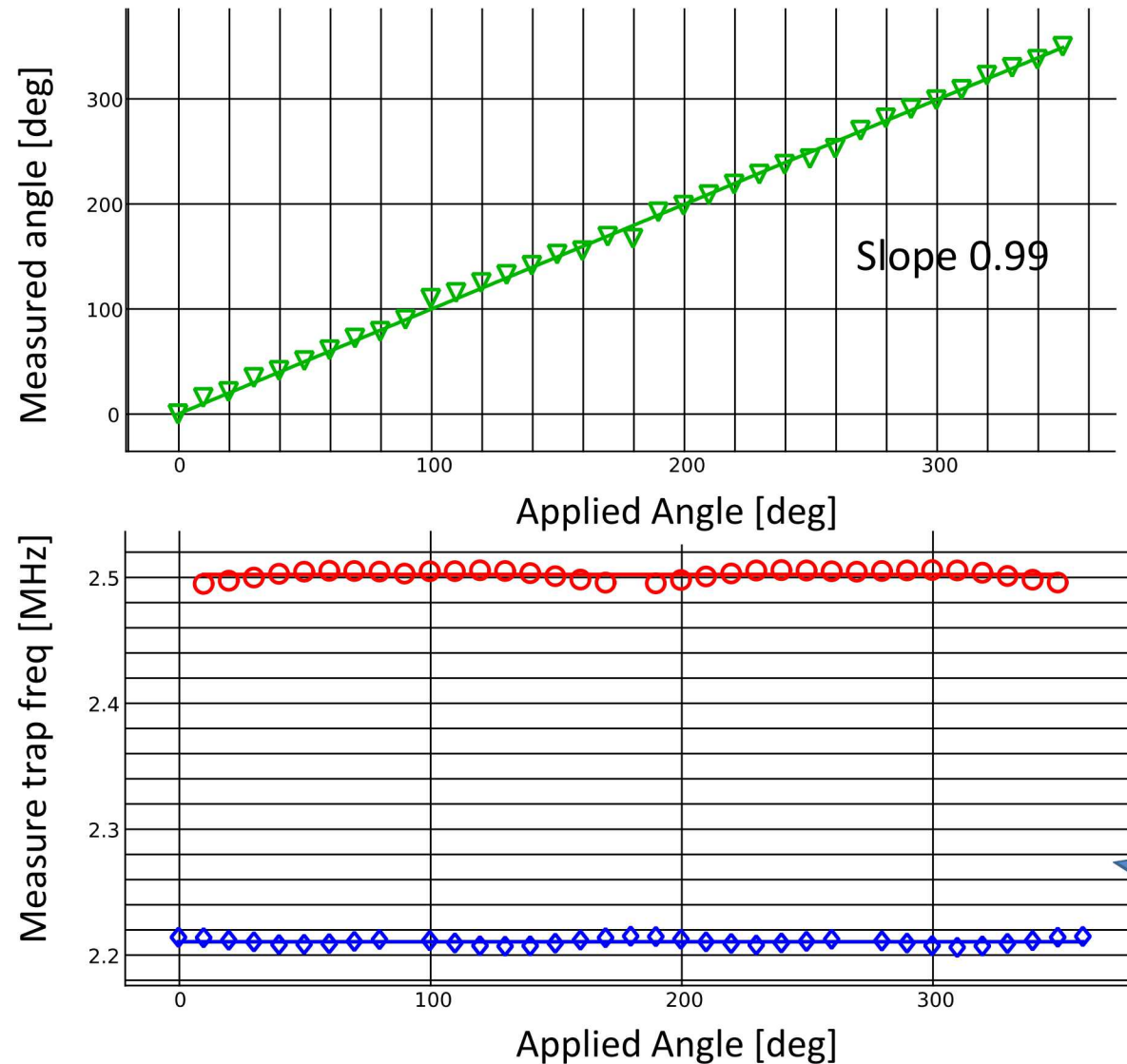
Advantages of parametric trapping solutions:

- Primitives are in terms of curvature tensor elements and can be applied at any location in the trap.
- Shuttling primitives can be easily combined

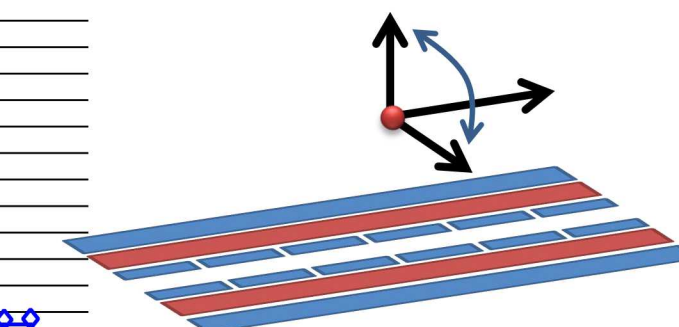
Example:

- Rotating ion crystal while translating through the trap

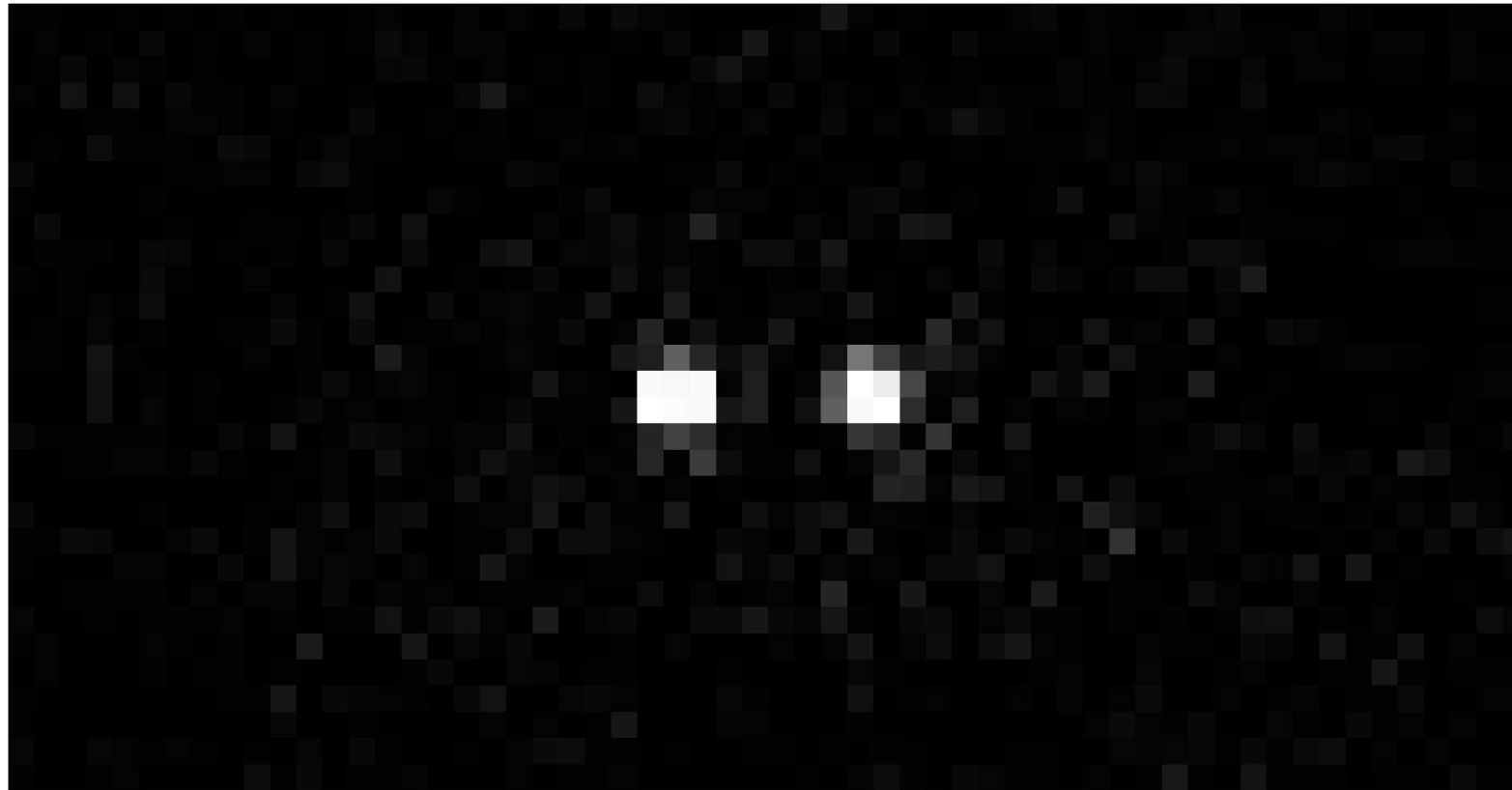
# Principal axes rotation



- Do we understand the trapping fields?
- Principal axes rotation realized as in simulation
- No change in trap frequencies

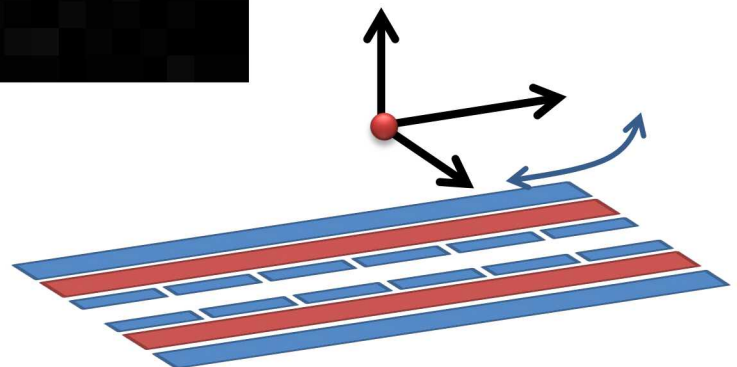


The simulations accurately describe the fields and curvatures generated by the trap

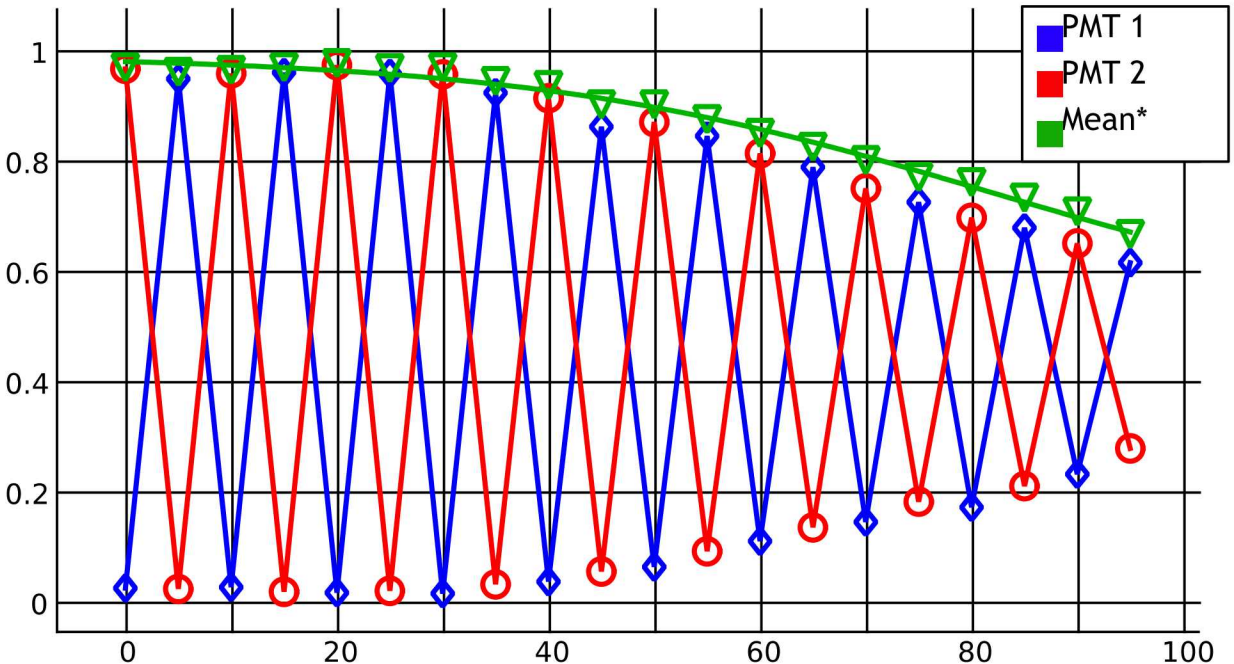
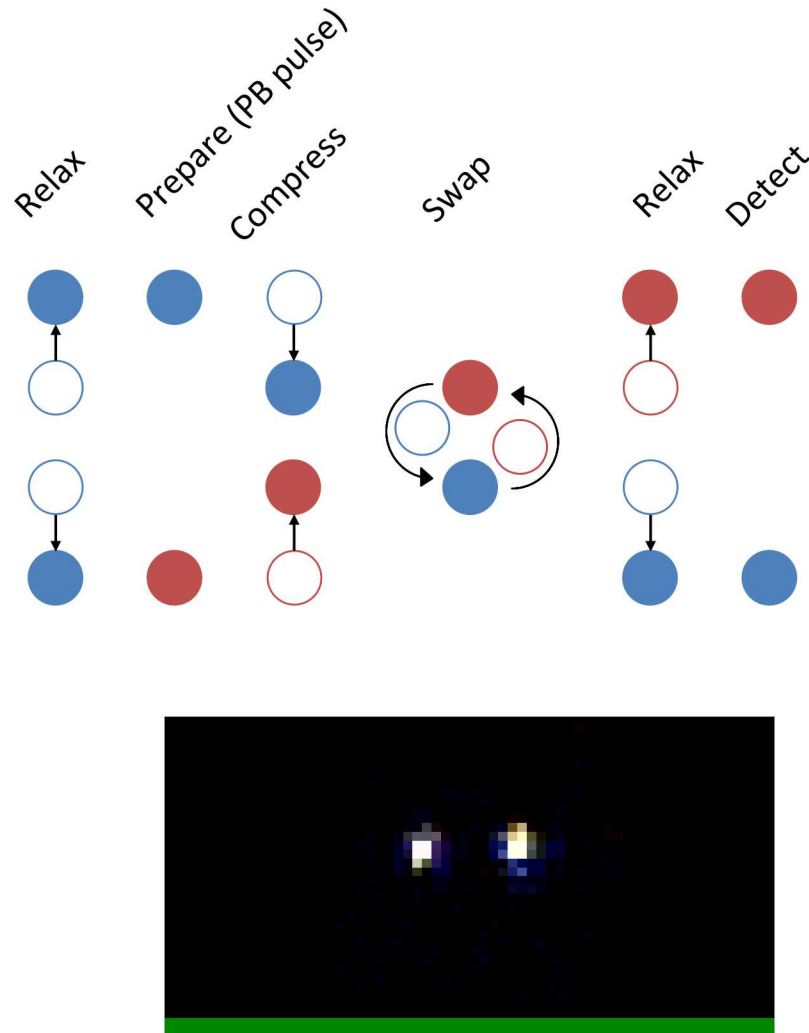


To be characterized as function of swapping time

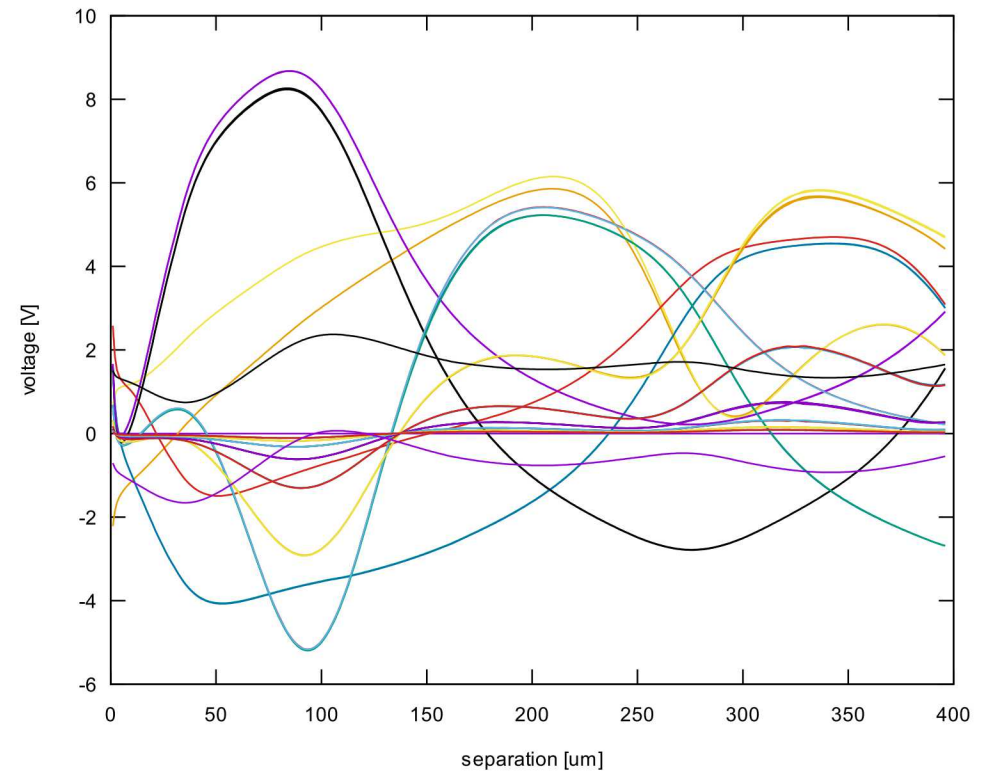
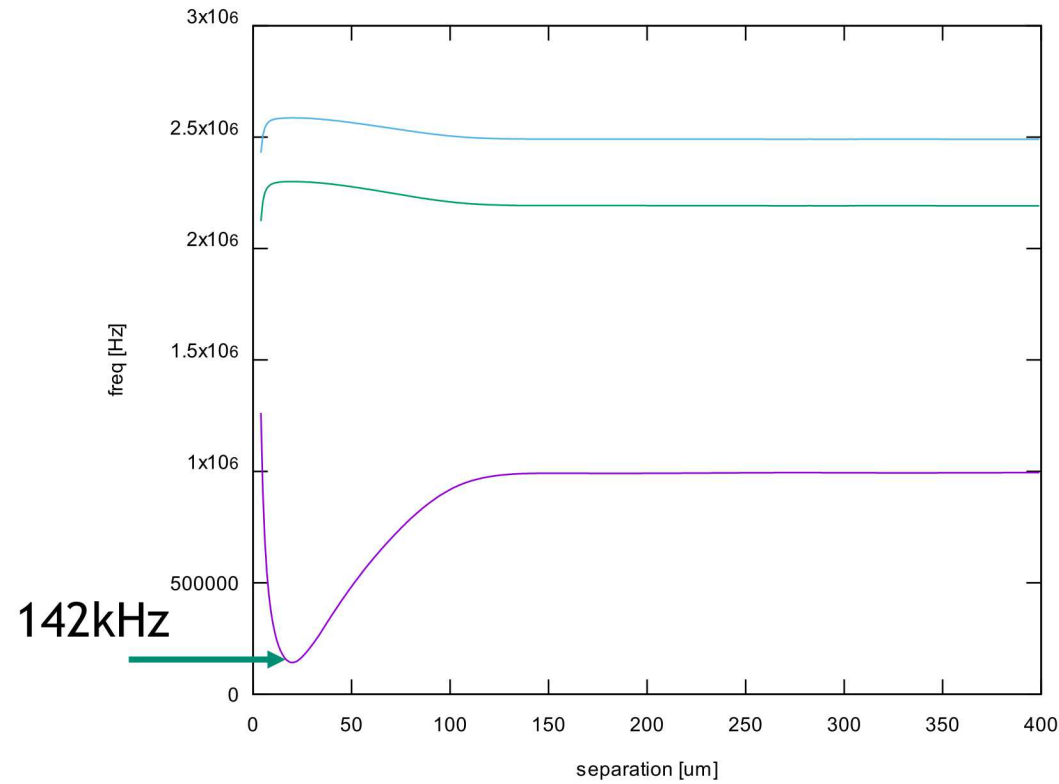
- Swapping fidelity
- Accumulated motion

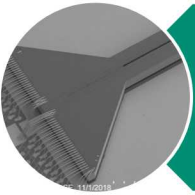


## Measuring swap fidelity

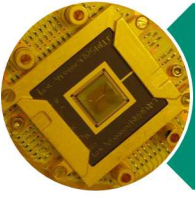


# Separation and merging of ions

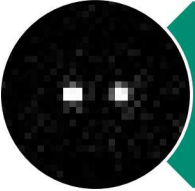




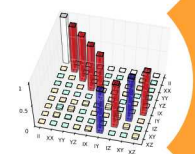
# Trap fabrication capabilities



HOA trap



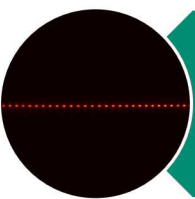
Classical control



Quantum operations

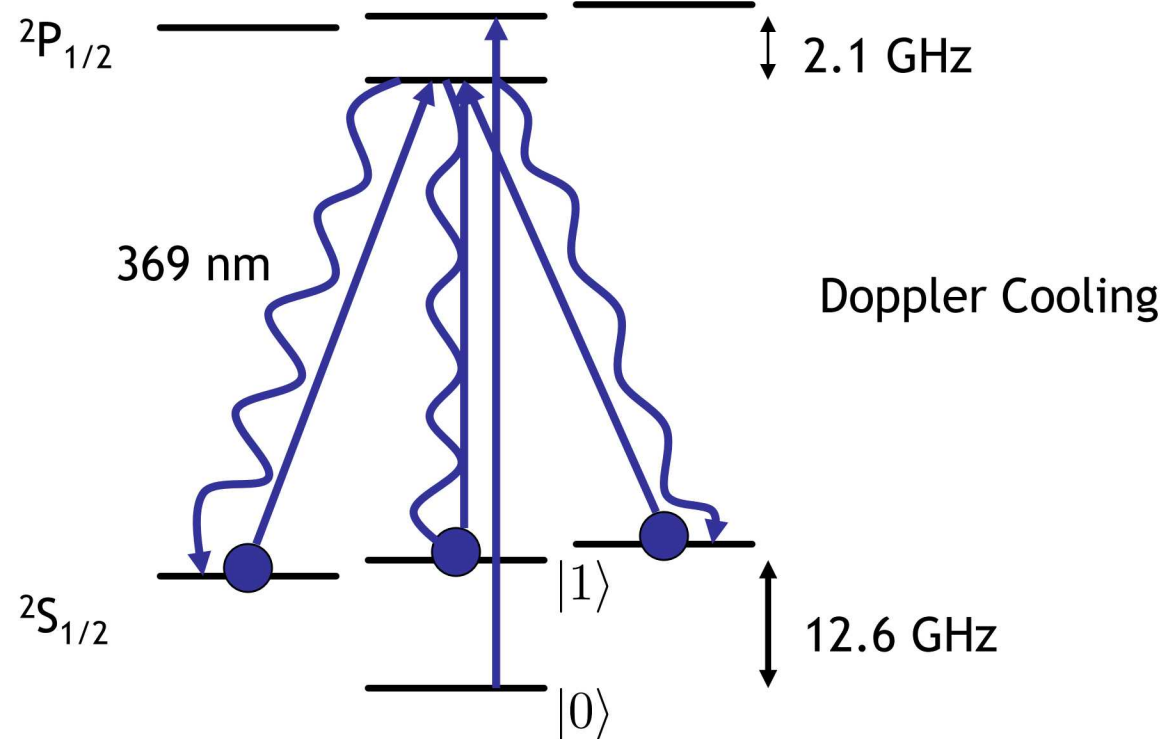


QSCOUT Quantum testbed



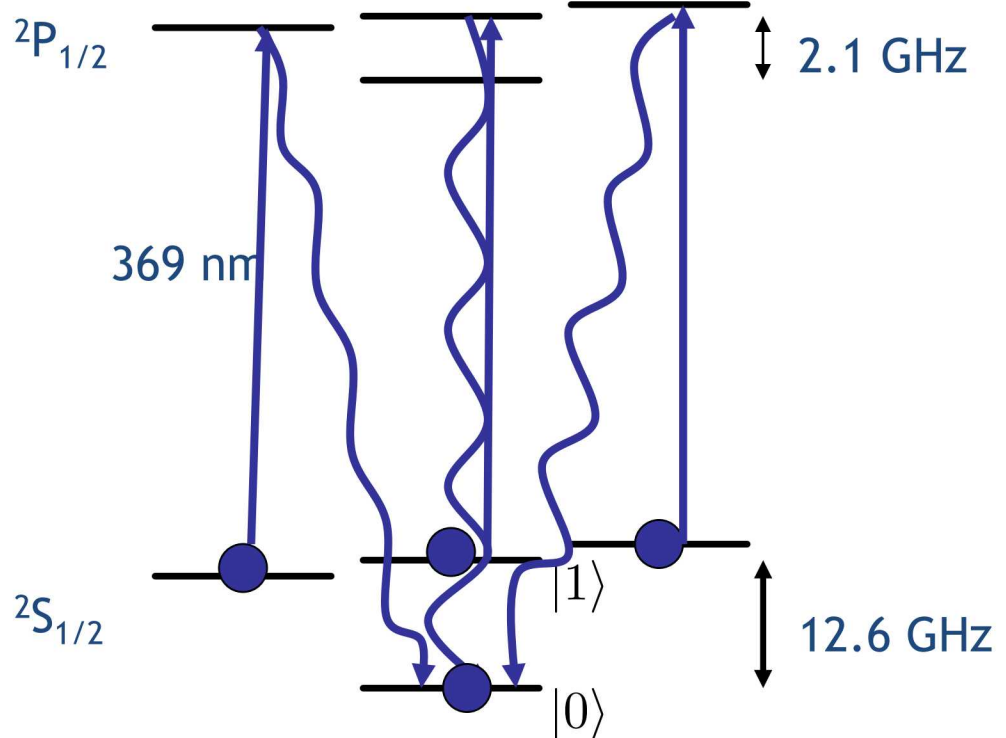
QSCOUT System engineering

# The Ytterbium Qubit



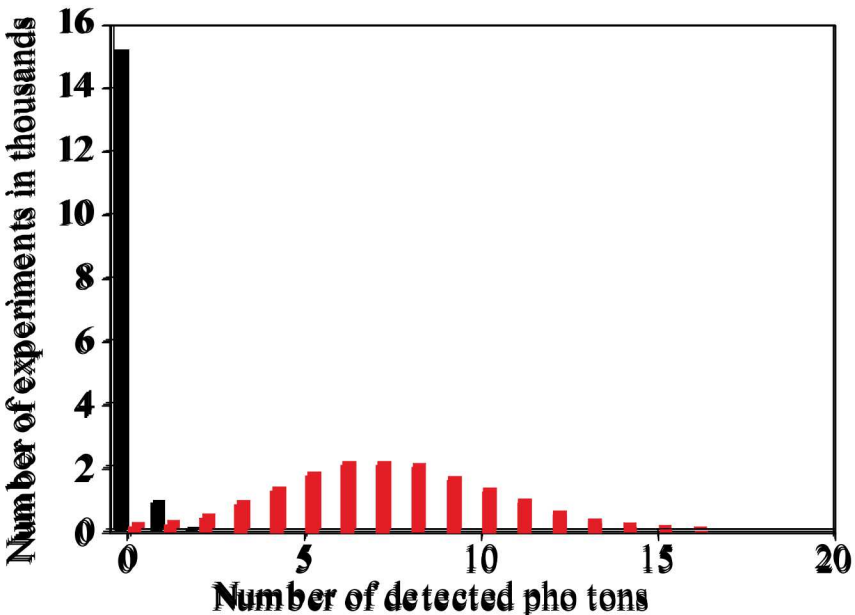
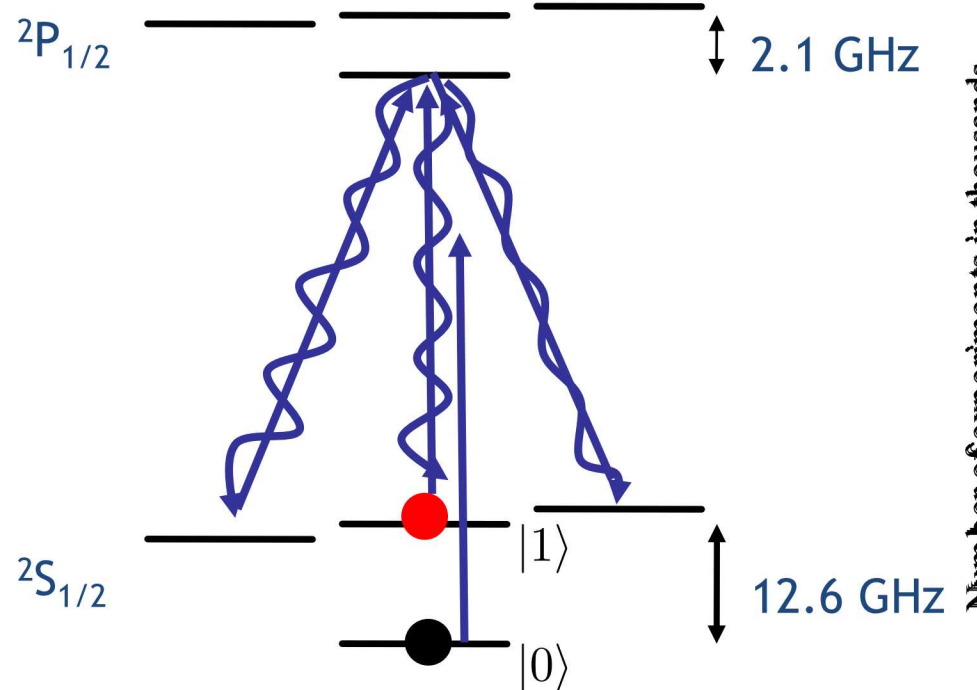
clock state qubit, magnetic field insensitive.

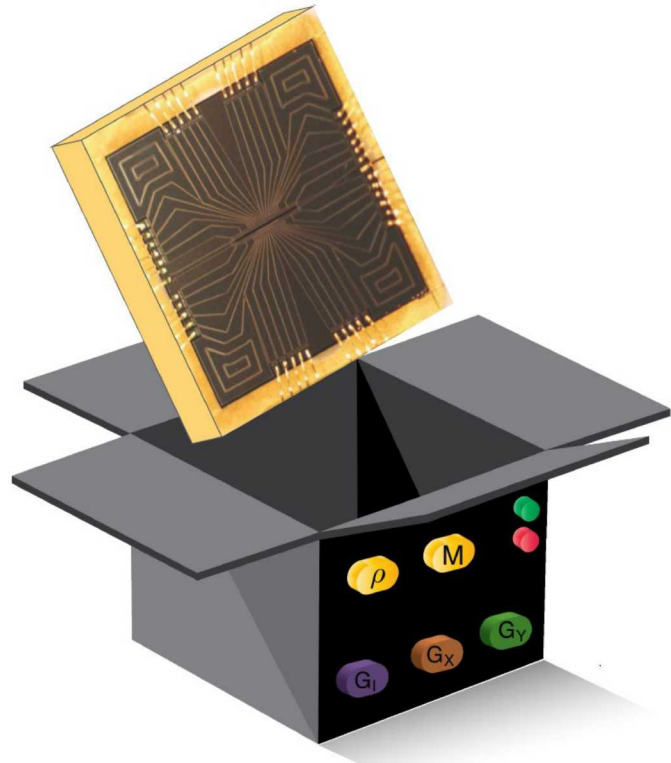
## state initialization



clock state qubit, magnetic field insensitive.

# $^{171}\text{Yb}^+$ state detection

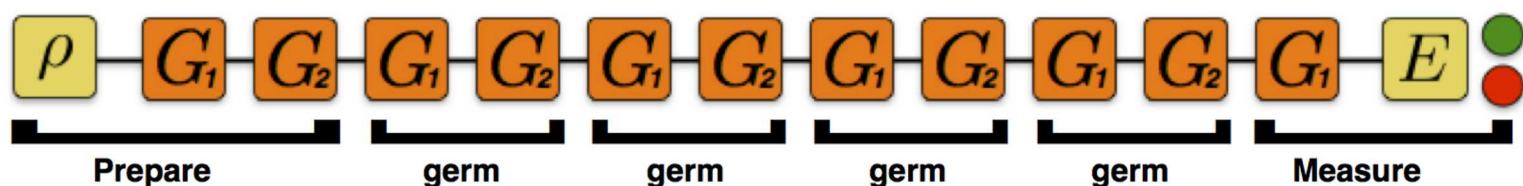




Developed at Sandia by  
QCVV team

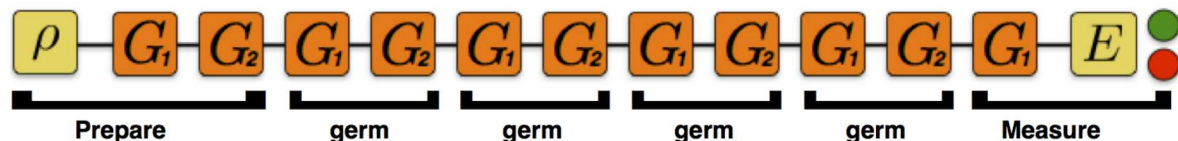
- No calibration required
- Detailed debug information
- Efficiently measures performance characterizing fault-tolerance (diamond norm)
- Detects non-Markovian noise

Uses structured sequences to amplify all possible errors



# GST sequences

Single qubit BB1 compensated microwave gates on  $^{171}\text{Yb}^+$



Desired “target” gates:

$G_i$  Idle (Identity)

$G_x$   $\pi/2$  rotation about  $x$ -axis

$G_y$   $\pi/2$  rotation about  $y$ -axis

Fiducials:

$\{\}$

$G_x$

$G_y$

$G_x \cdot G_x$

$G_x \cdot G_x \cdot G_x$

$G_y \cdot G_y \cdot G_y$

Germs:

$G_i$

$G_x \cdot G_y$

$G_x \cdot G_y \cdot G_i$

$G_x \cdot G_i \cdot G_y$

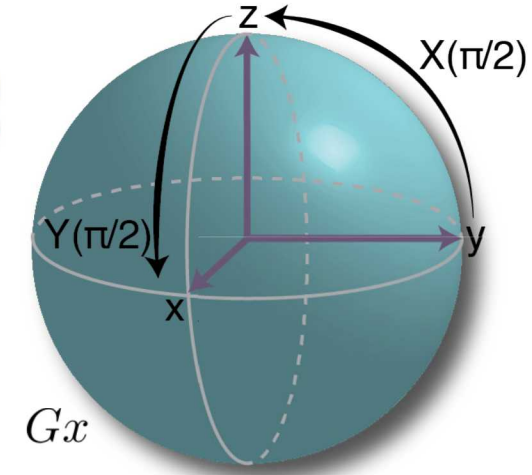
$G_x \cdot G_i \cdot G_i$

$G_y \cdot G_i \cdot G_i$

$G_x \cdot G_x \cdot G_i \cdot G_y$

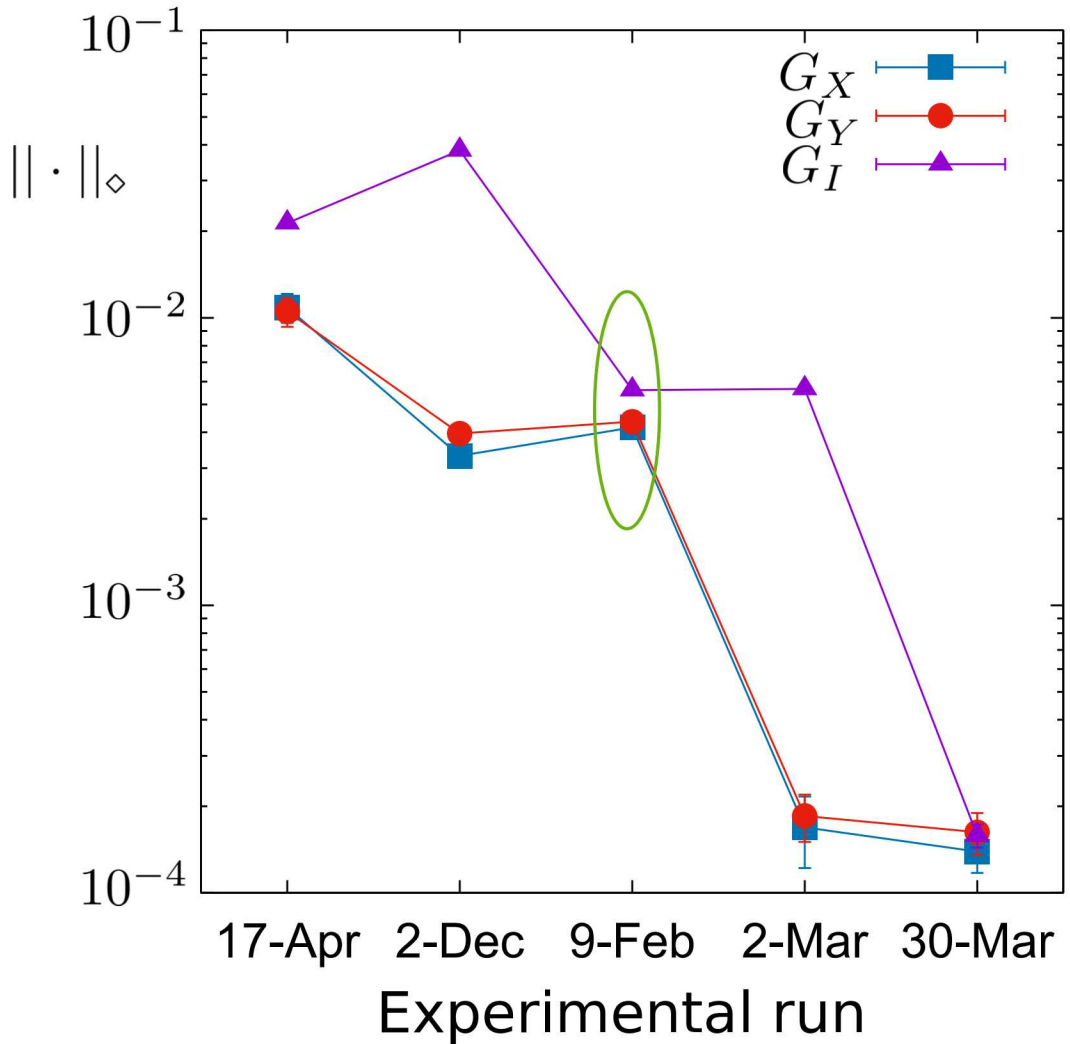
Approximately prepare 6 points on Bloch sphere  $G_x \cdot G_y \cdot G_y \cdot G_i$

$G_x \cdot G_x \cdot G_y \cdot G_x \cdot G_y \cdot G_y$



# GST: debugging microwave gates

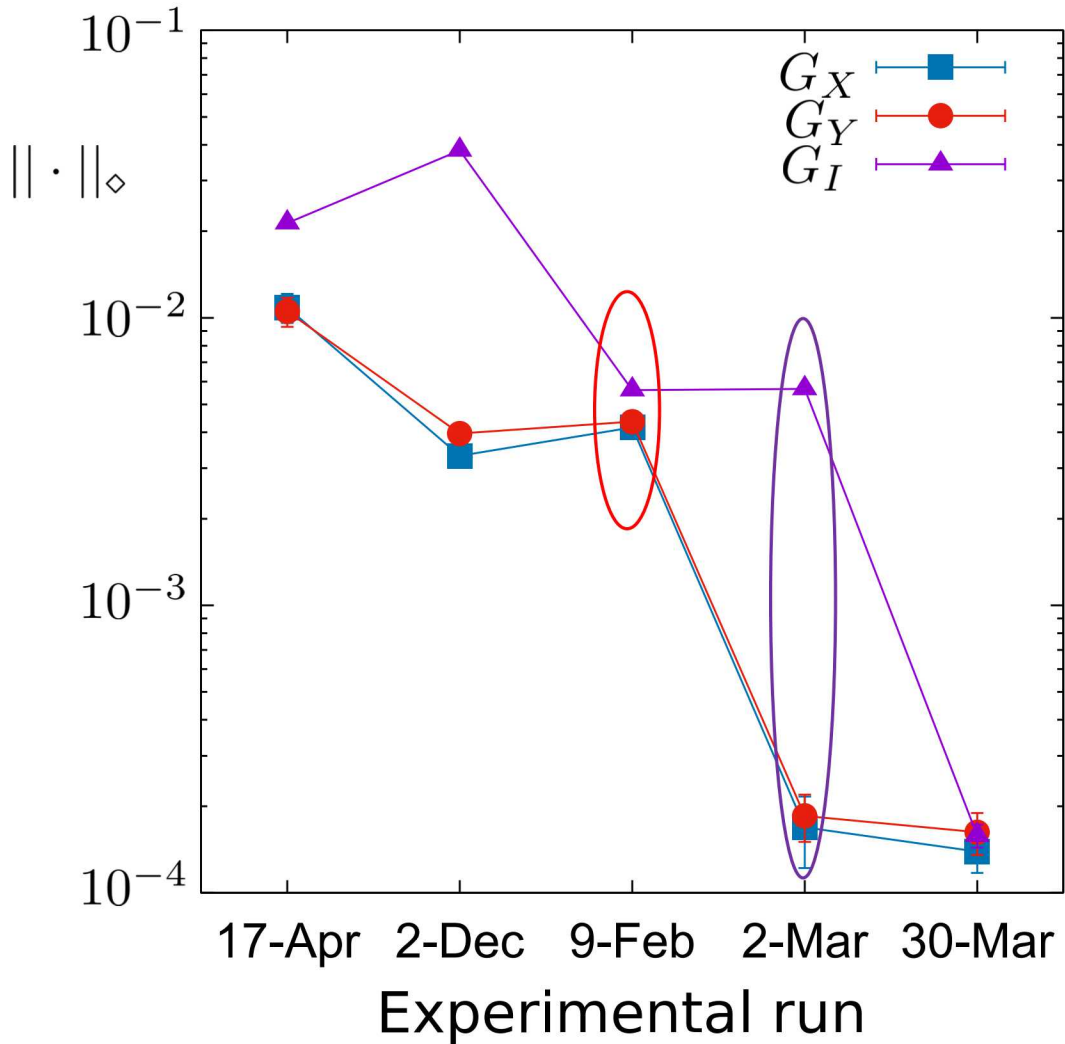
Gate	Rotn. axis	Angle
$G_I$	0.5252	
	-0.009	
	0.8506	
	-0.0244	$0.001699\pi$
$G_X$	$-3 \times 10^{-6}$	
	-1	
	$-3 \times 10^{-5}$	$0.501308\pi$
	-0.009	
$G_Y$	-0.2474	
	0.0001	
	0.9689	
	-0.0001	$0.501366\pi$

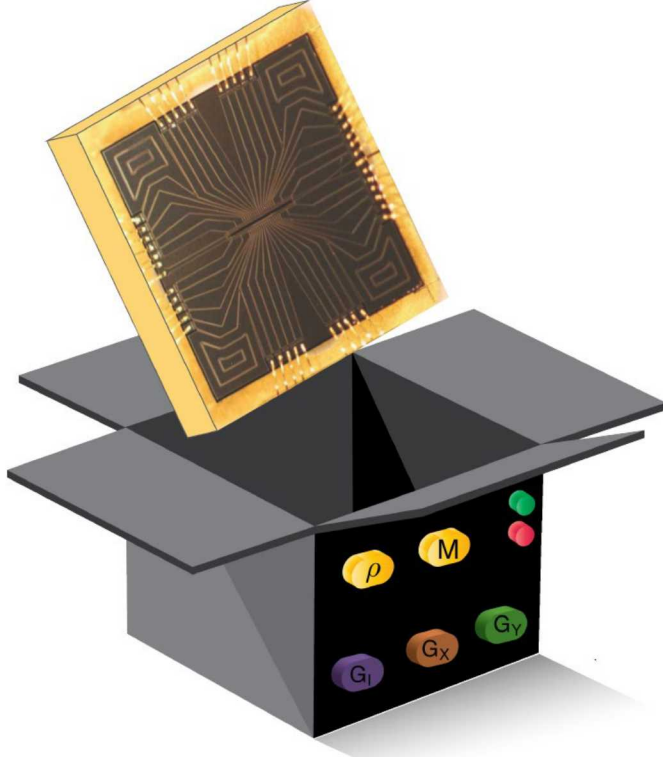


# GST: debugging microwave gates

Gate	Rotn. axis	Angle
$G_I$	0.5252	
	-0.009	
	0.8506	
	-0.0244	$0.001699\pi$
$G_X$	$-3 \times 10^{-6}$	
	-1	
	$-3 \times 10^{-5}$	$0.501308\pi$
	-0.009	
$G_Y$	-0.2474	
	0.0001	
	0.9689	
	-0.0001	$0.501366\pi$

Gate	Rotn. axis	Angle
$G_I$	-0.0035	
	0.014	
	-0.9999	
	0.0006	$0.001769\pi$
$G_X$	$-3 \times 10^{-5}$	
	-1	
	$1 \times 10^{-4}$	$0.500007\pi$
	0.0006	
$G_Y$	0.1104	
	$4 \times 10^{-5}$	
	0.9939	
	0.0005	$0.50001\pi$





Assumptions:

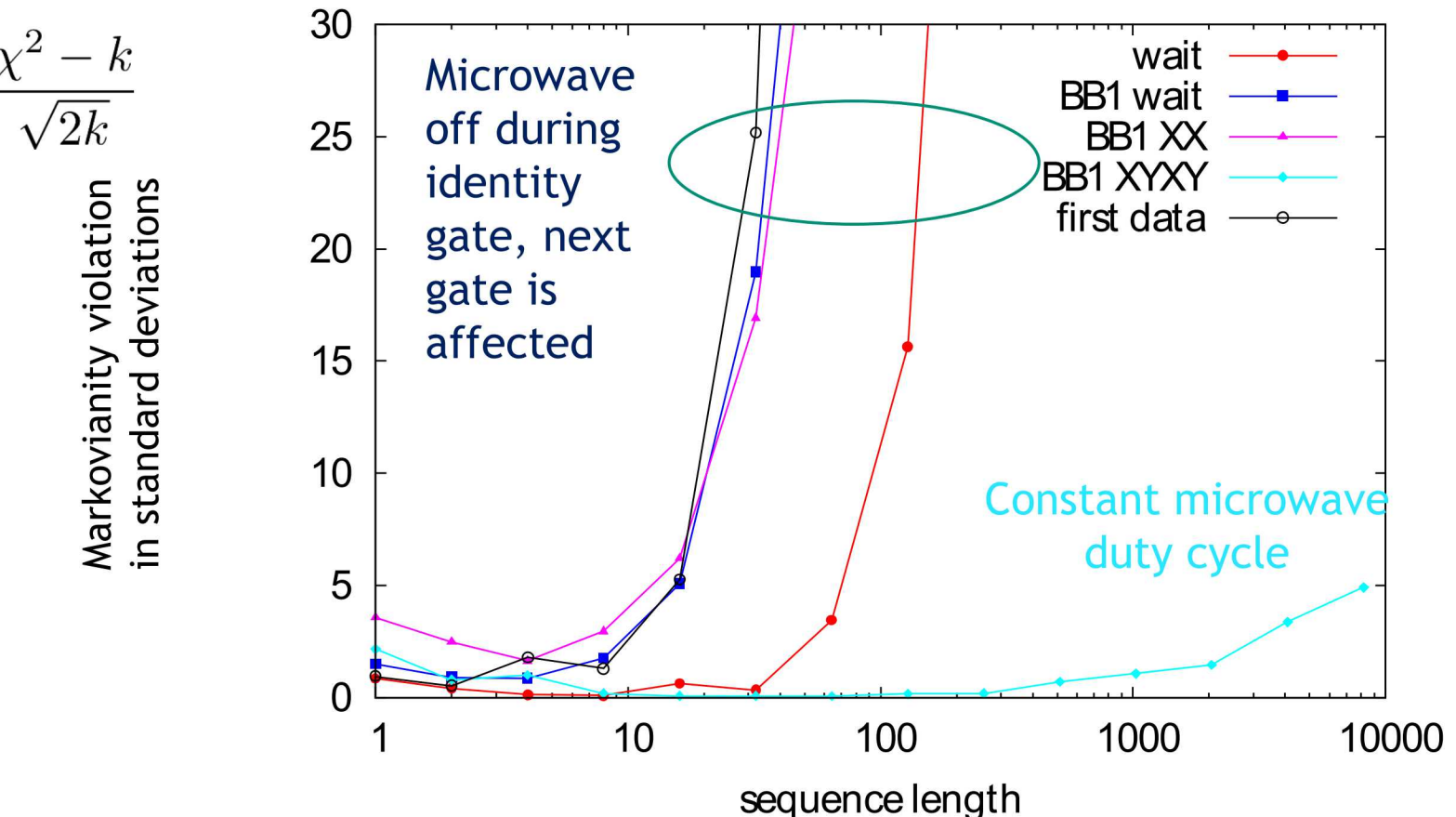
- Qubits in a box
- Pressing a button always executes the exactly same operation
- Independent from context (gates executed before)
- Independent from when a gate is executed

GST uses a large (over-complete) number of sequences.

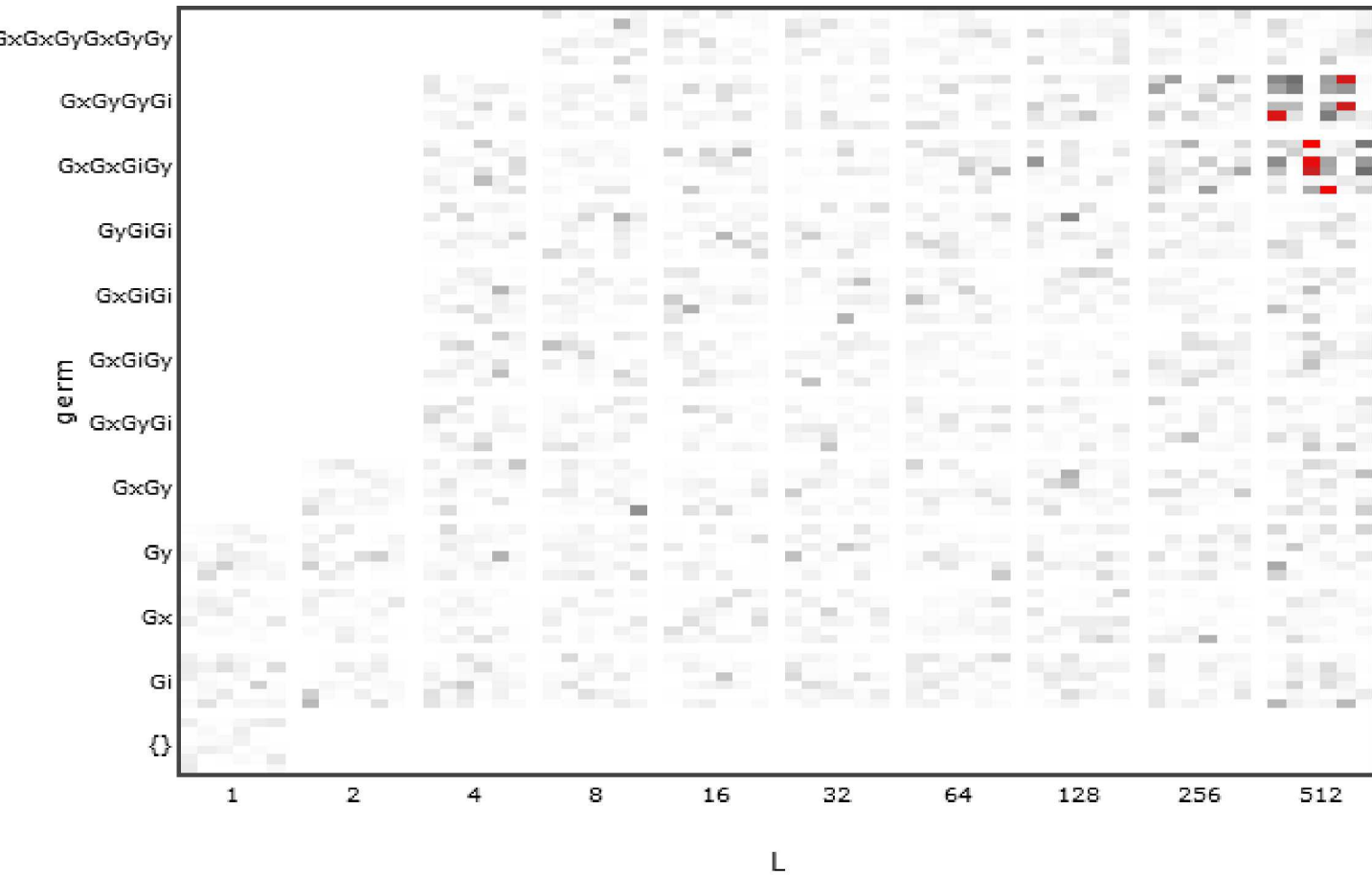
We can look whether the assumptions are satisfied

Ongoing work to improve and distinguish detection of context and time dependence of classical control

The  $\chi^2$  values from the fits are expected to follow a  $\chi^2$  distribution with mean  $k$  and standard deviation  $\sqrt{2k}$



BB1 decoupled gates with decoupled identity have very small non-Markovian noise



- Identifying problems due to context dependency and drift

- Red boxes show sequences which violate the Markovian model
- For a Markovian realization with 95% probability there are no red boxes
- These sequences show context dependency of gates
- X- and Y- gates behave differently if applied after an I gate

Best results for microwave single qubit gates:

- BB1 dynamically compensated pulse sequences
- Decoupling sequence for identity gate
- Drift control for  $\pi$ -time and qubit frequency

95% confidence intervals

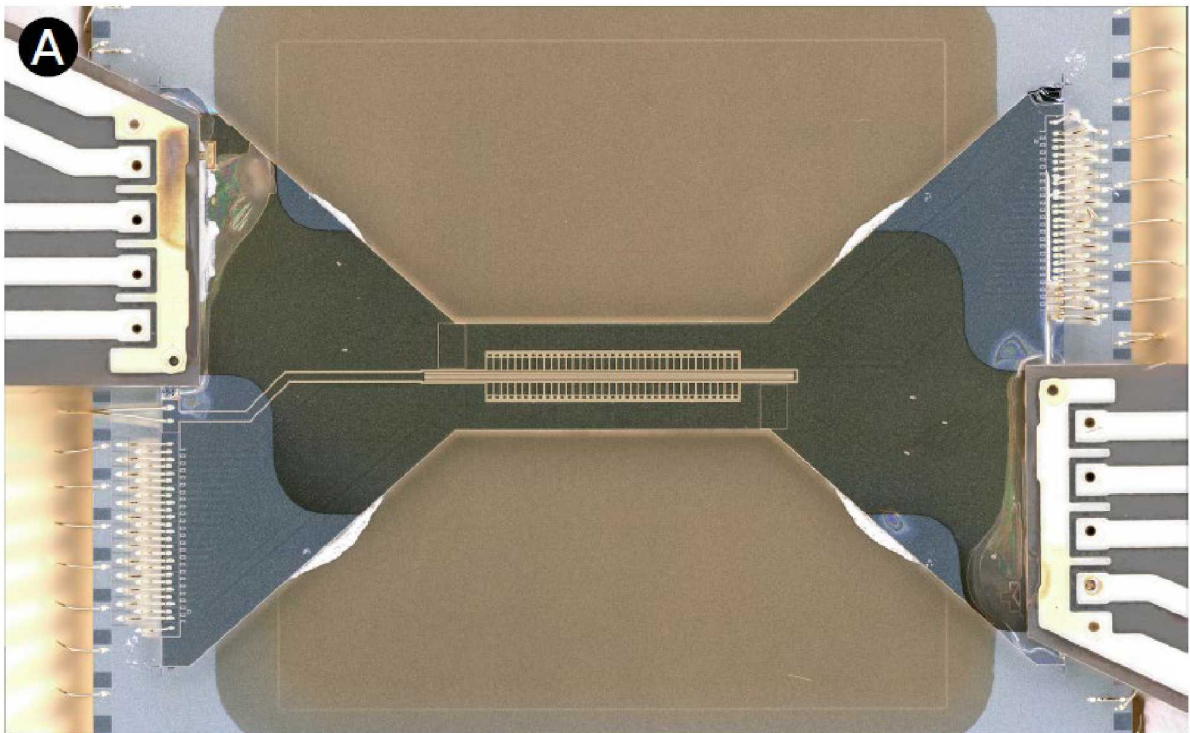
Gate	Process Infidelity	$1/2 \diamond$ -Norm
$G_I$	$6.9(6) \times 10^{-5}$	$7.9(7) \times 10^{-5}$
$G_X$	$6.1(7) \times 10^{-5}$	$7.0(15) \times 10^{-5}$
$G_Y$	$7.2(7) \times 10^{-5}$	$8.1(15) \times 10^{-5}$

All gates are better than the fault tolerance threshold of  $9.7 \times 10^{-5}$   
P. Aliferis and A. W. Cross, Phys. Rev. Lett. 98, 220502 (2007).

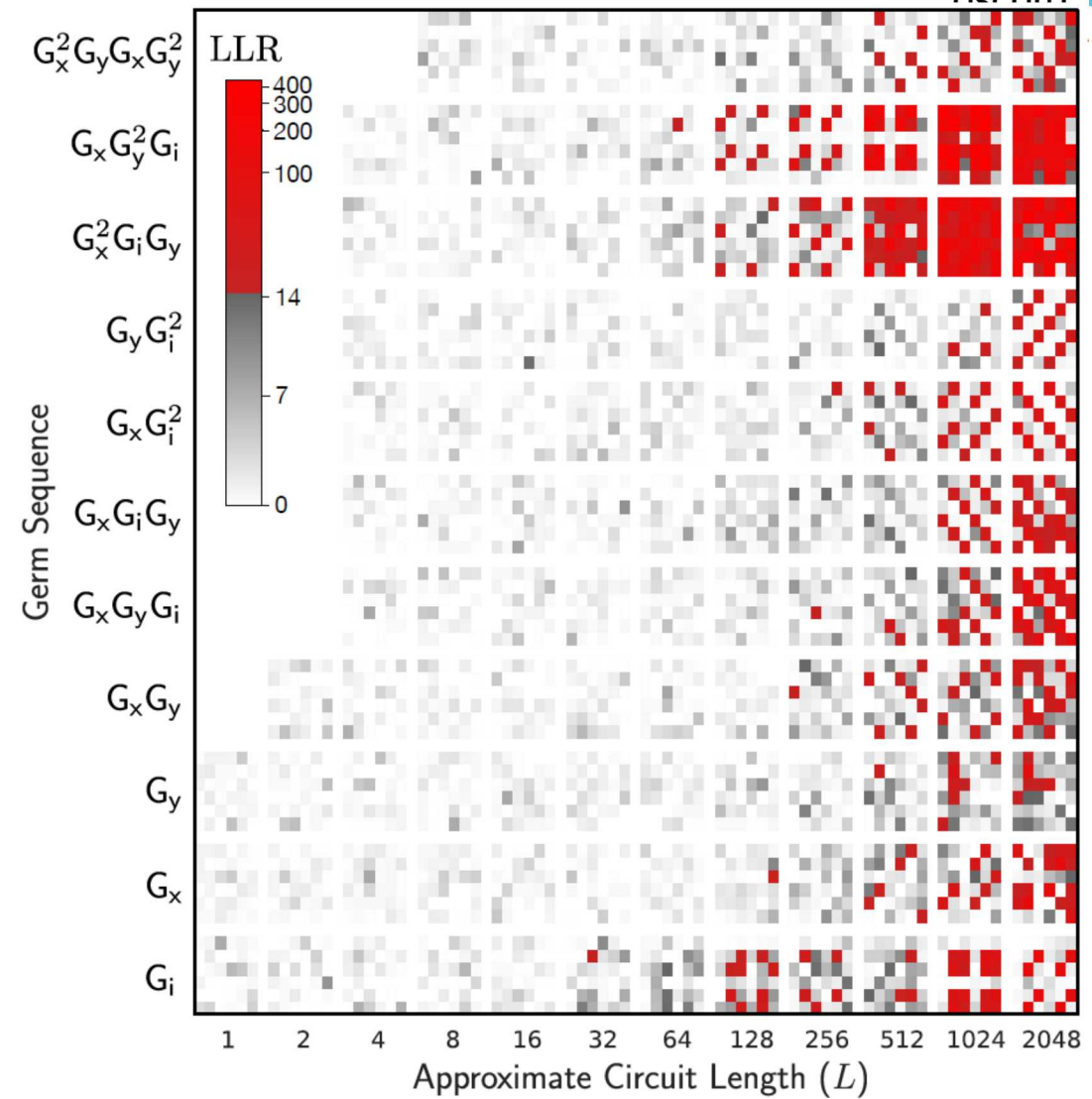
# Challenge: Model violation in GST

Assumptions are that gate actions are

- Independent of surrounding gates (context dependency)
- Independent of time (drift)



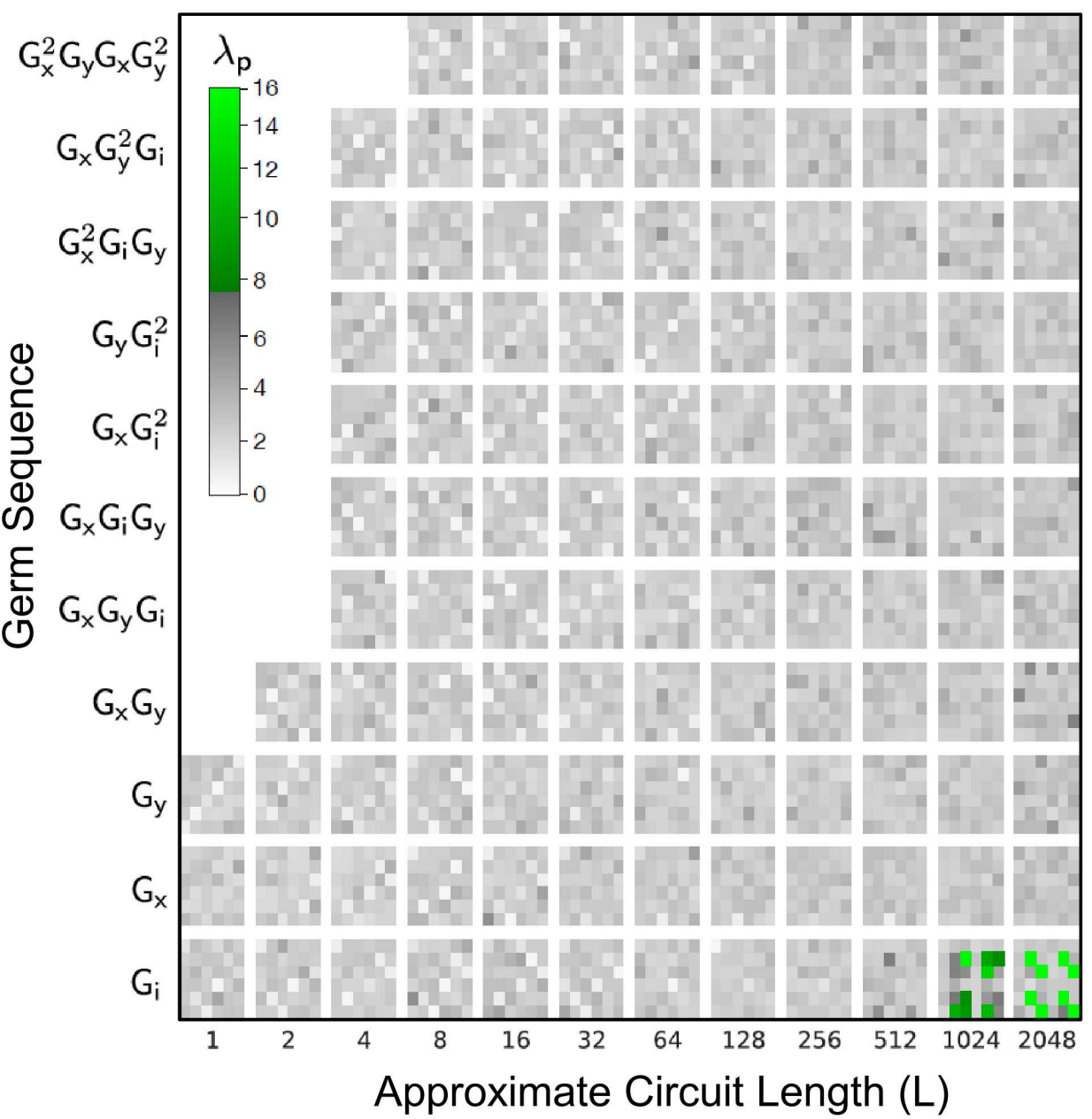
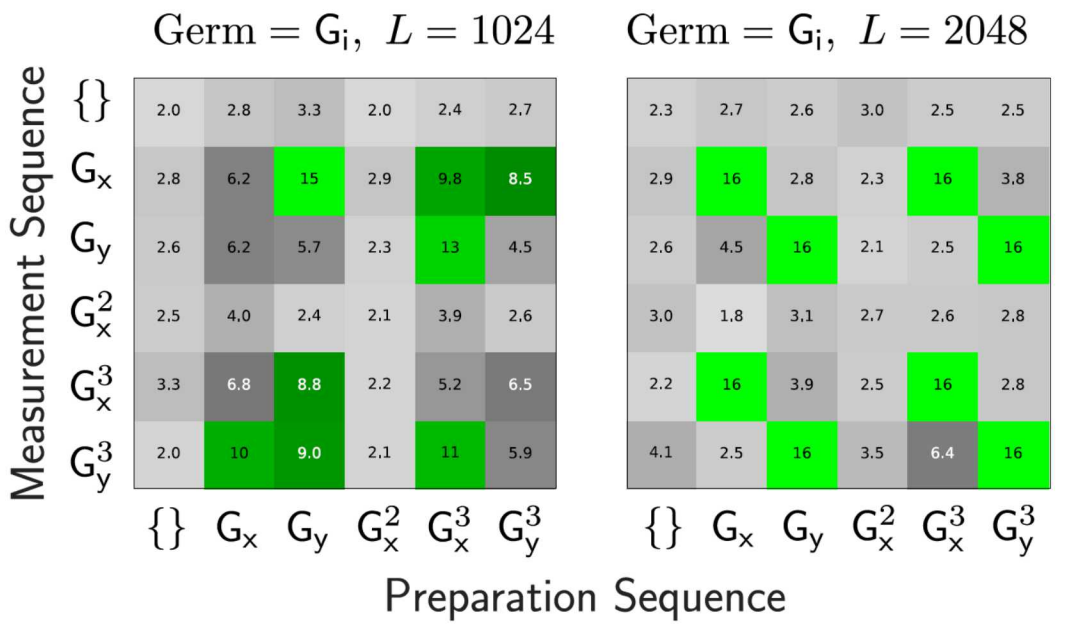
Experiments: Single-qubit microwave gates in trap with integrated microwave antenna



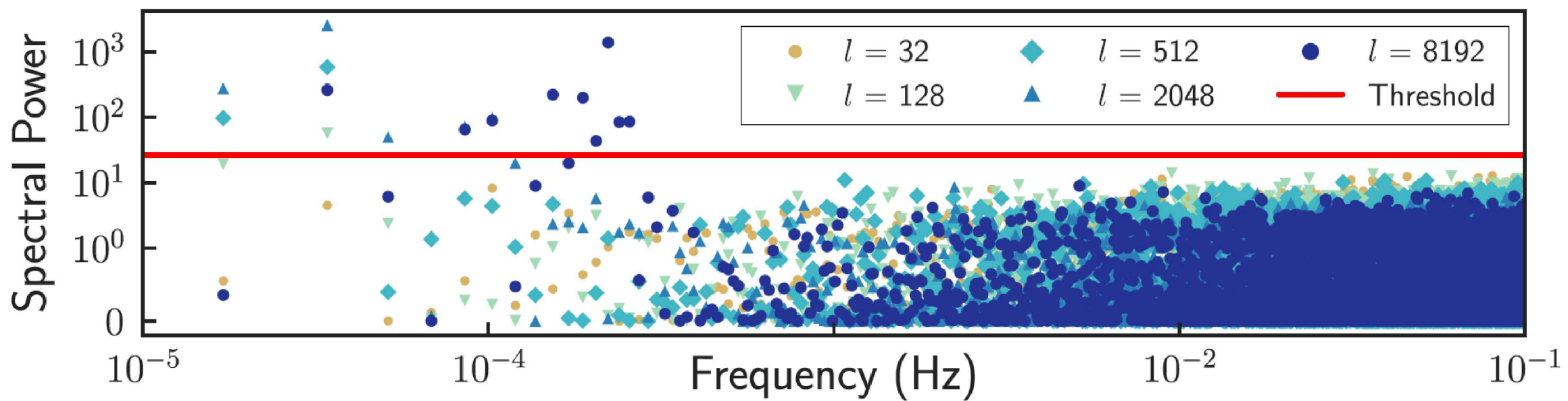
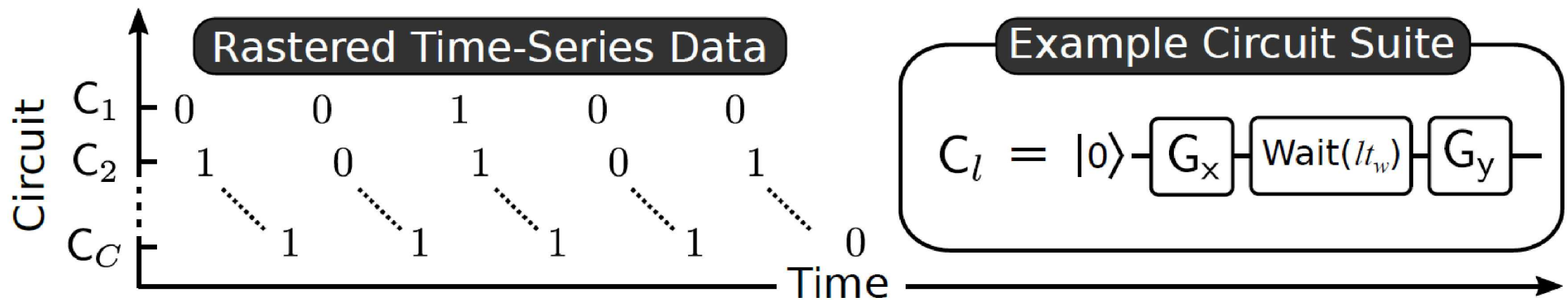
Model violation for time-independent GST estimate.  
(Log-likelihood ratio) global significance 5%

# Is there drift?

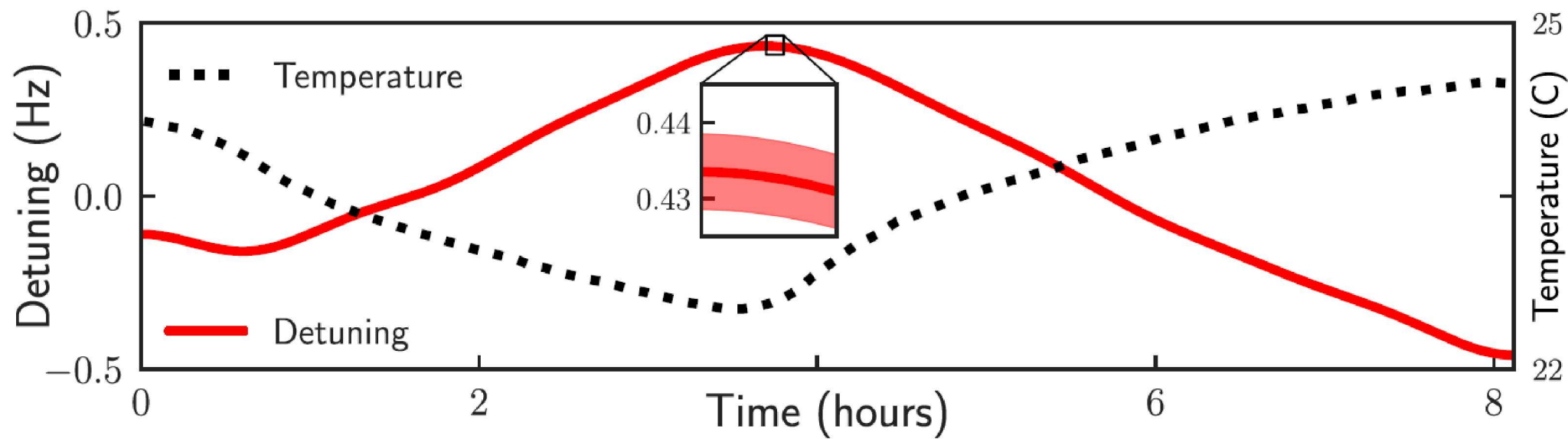
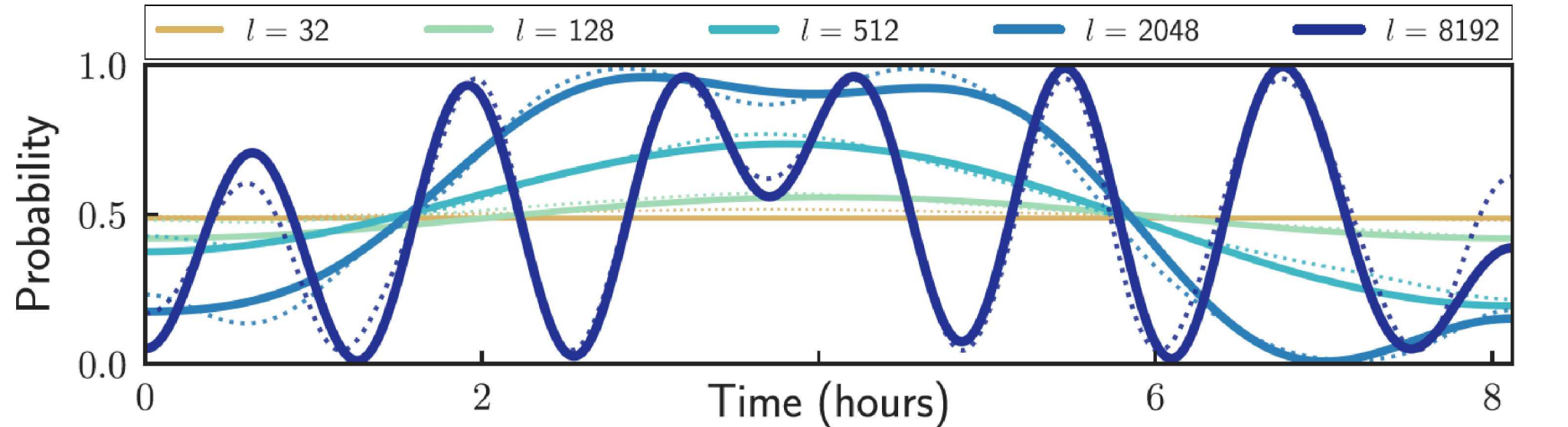
- Time-resolved GST characterization
- Ramsey experiments show significant drift
- These sequences are candidates for further investigation



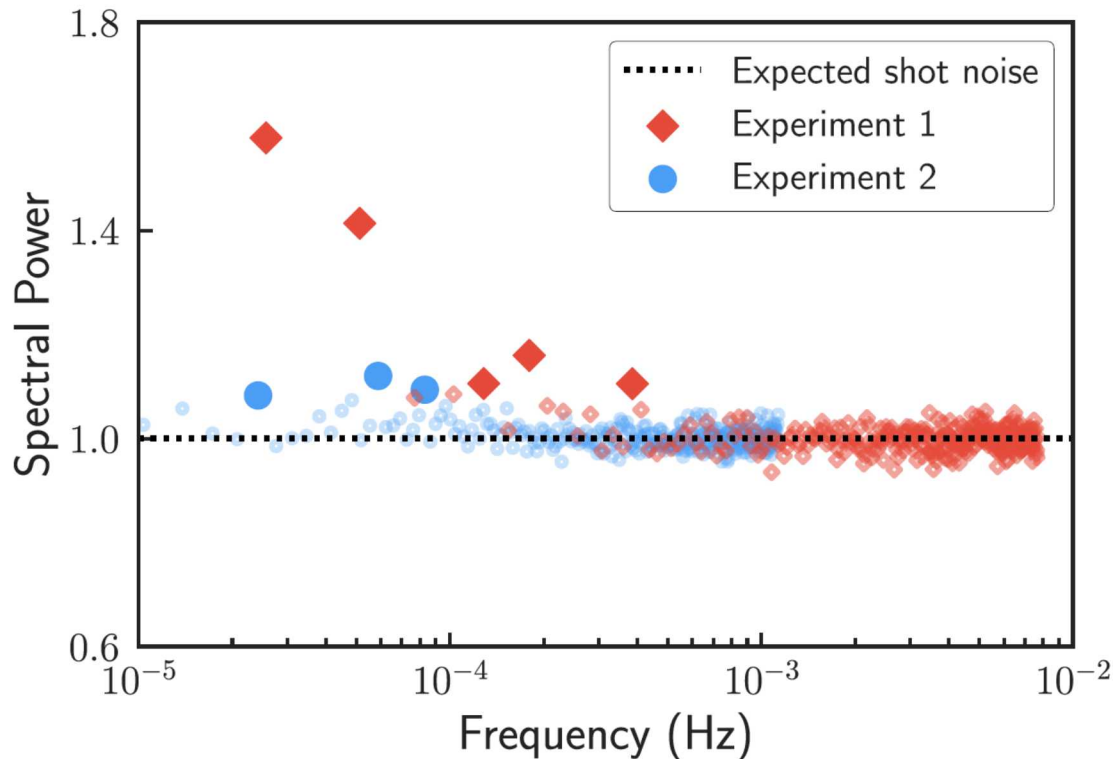
$\lambda_p = -\log_{10}(p)$  where  $p$  is the p-value of the largest power in the spectrum for that circuit



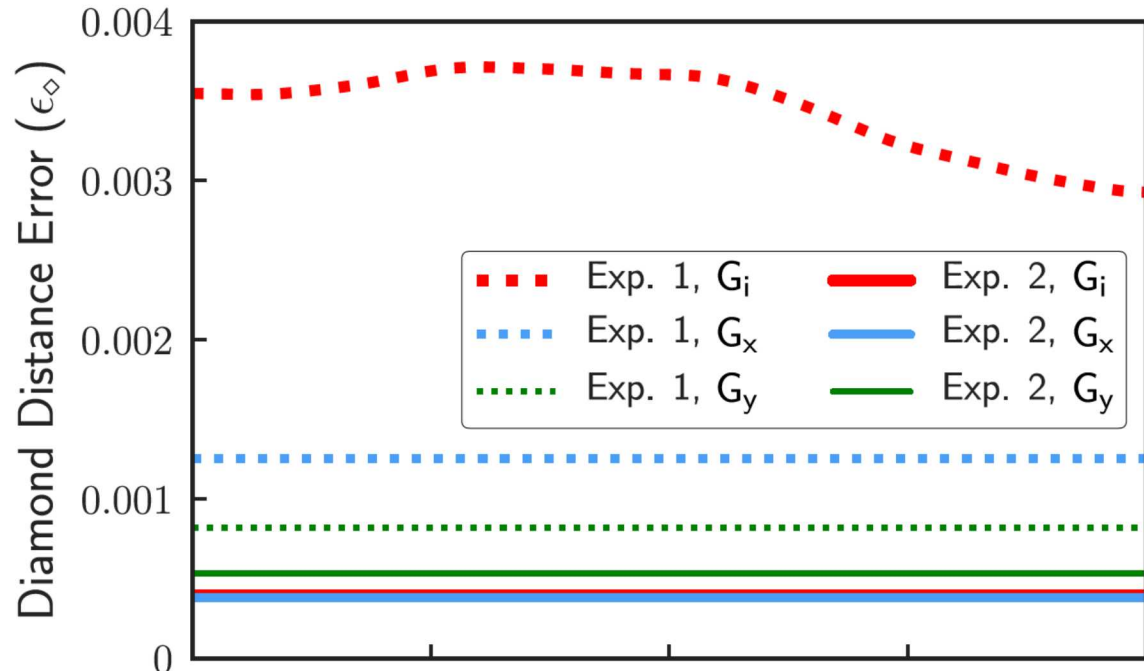
# Can the drifting parameter be reconstructed?



# Experimental Improvements



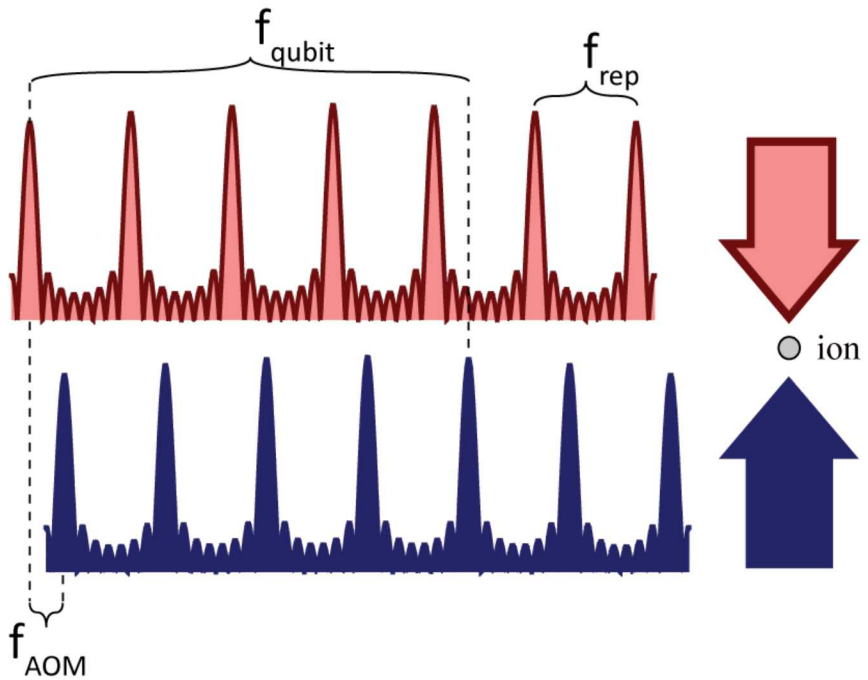
- Spectral power averaged over all sequences
- Small residual drift, cannot be assigned to specific sequences
- Reconstruction of individual sequences is below statistical significance



## Improvements:

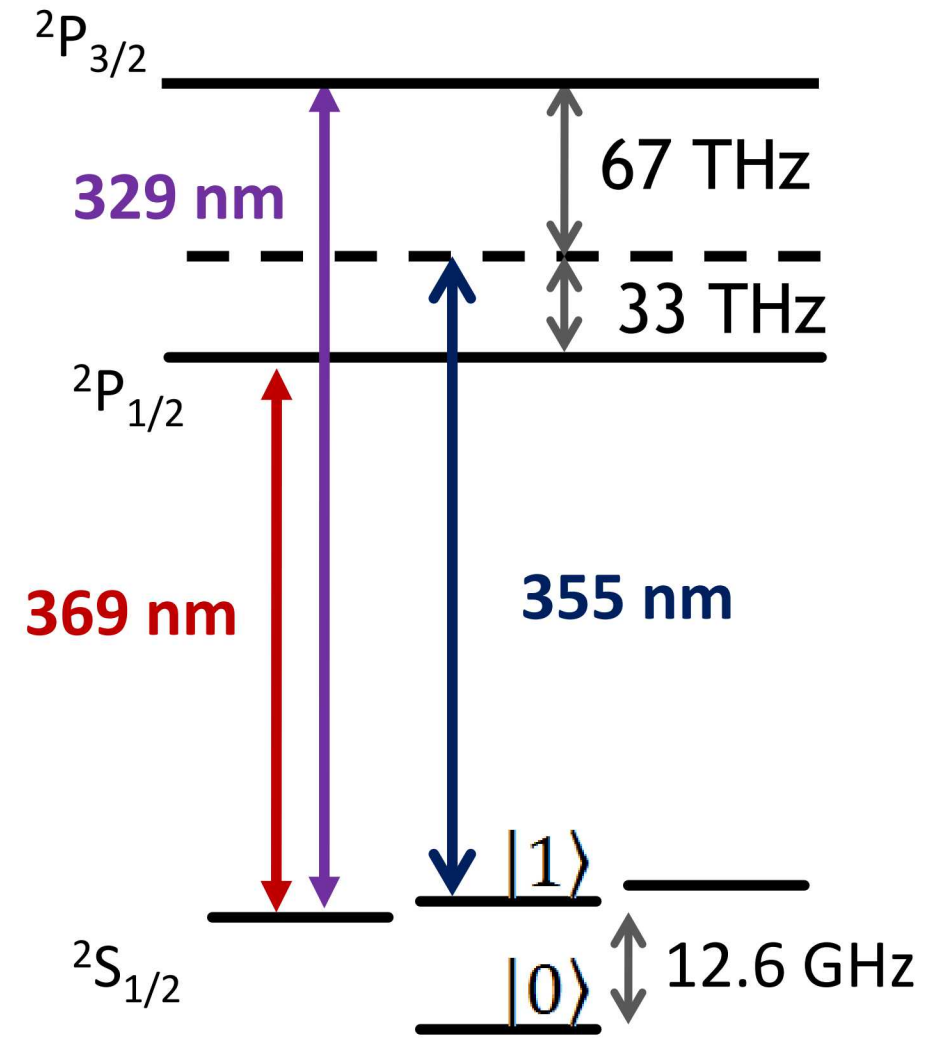
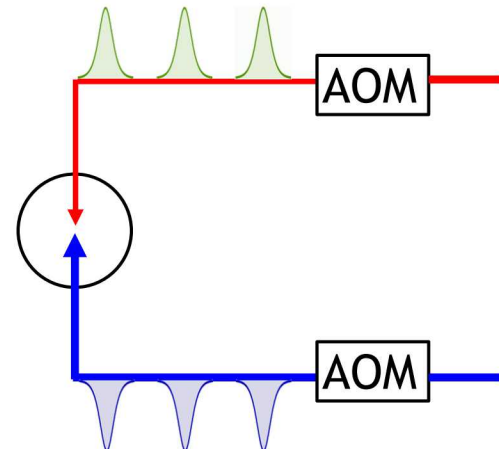
- Stabilized room temperature
- Incorporated drift control – feedback on transition frequency and  $\pi$ -time.

# 355 Raman transitions: $^{171}\text{Yb}^+$



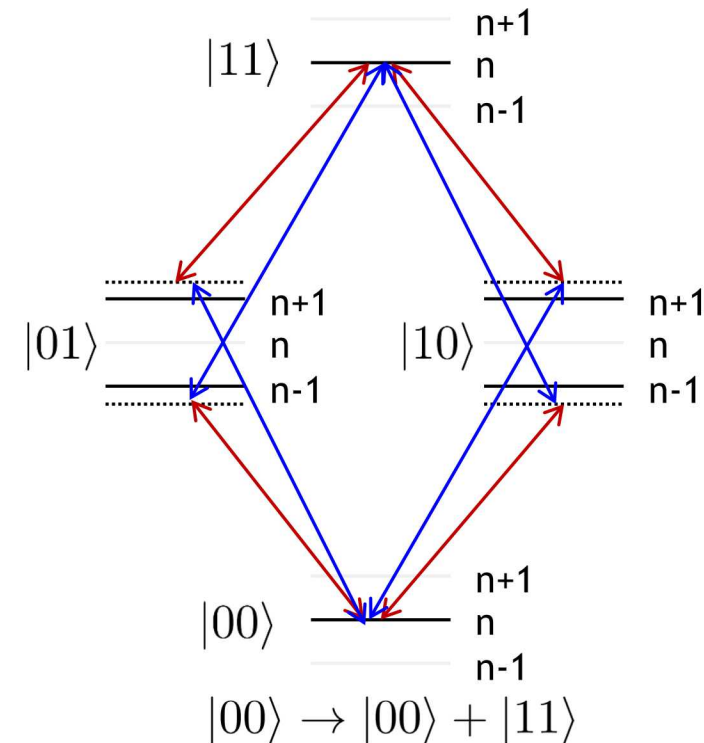
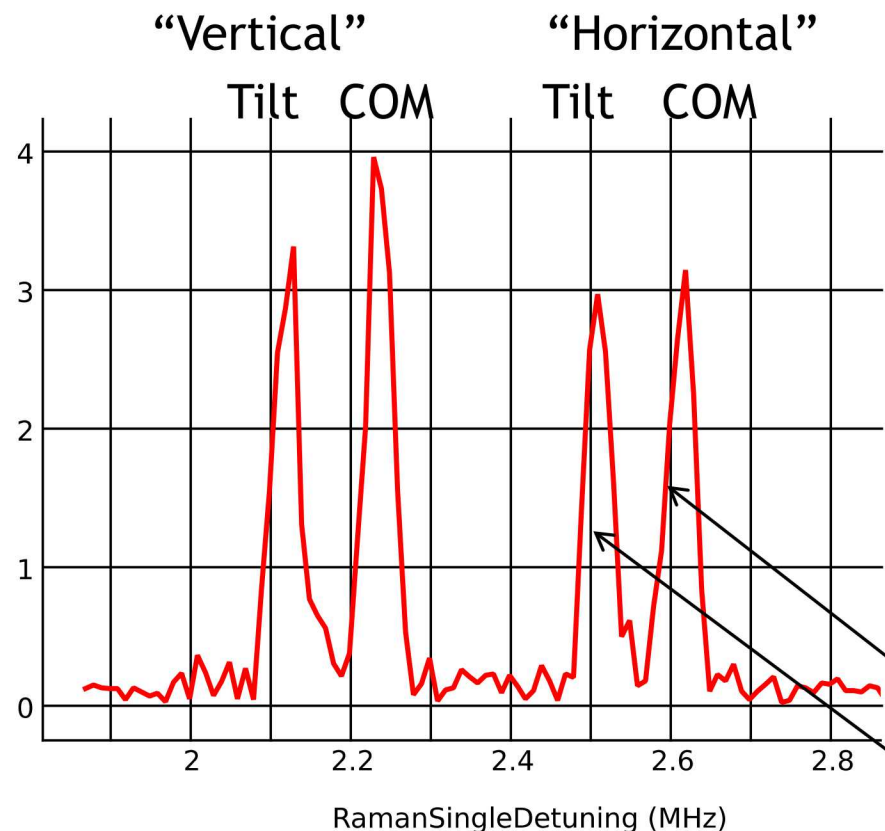
Requirement:

$$f_{\text{qubit}} = n f_{\text{rep}} \pm f_{\text{AOM}}$$



# Two-qubit gate implementation

- Mølmer-Sørensen gates [1] using 355nm pulsed laser
- All two-qubit gates implemented using Walsh compensation pulses [2]



Heating rates

$\approx 60$  quanta/s

$< 8$  quanta/s

[1] K. Mølmer, A. Sørensen, PRL 82, 1835 (1999)

[2] D. Hayes et al. Phys. Rev. Lett. 109, 020503 (2012)



## Two-qubit gate characterization

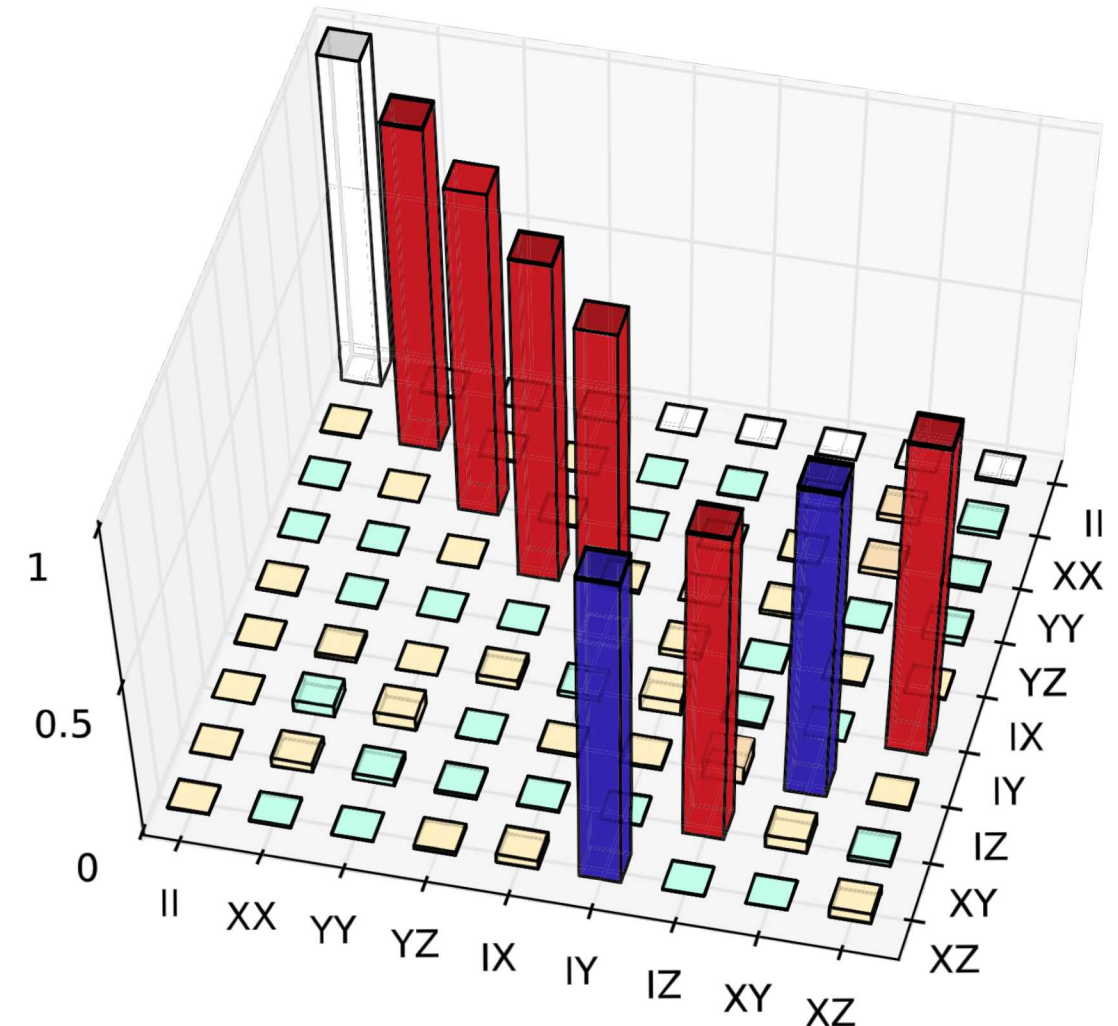
Gate	Process infidelity	$\frac{1}{2}$ Diamond norm
$G_I$	$1.6 \times 10^{-3} \pm 1.6 \times 10^{-3}$	$28 \times 10^{-3} \pm 7 \times 10^{-3}$
$G_{XX}$	$0.4 \times 10^{-3} \pm 1.0 \times 10^{-3}$	$27 \times 10^{-3} \pm 5 \times 10^{-3}$
$G_{YY}$	$0.1 \times 10^{-3} \pm 0.9 \times 10^{-3}$	$26 \times 10^{-3} \pm 4 \times 10^{-3}$
$G_{MS}$	$4.2 \times 10^{-3} \pm 0.6 \times 10^{-3}$	$38 \times 10^{-3} \pm 5 \times 10^{-3}$

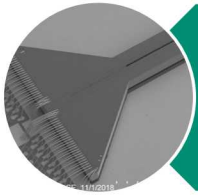
95% confidence intervals

**Process fidelity of two-qubit Mølmer-Sørensen gate  $> 99.5\%$**

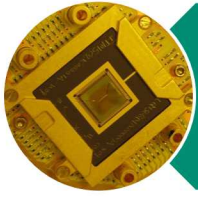
The best characterized two qubit gate

By the way: It's in a scalable surface trap

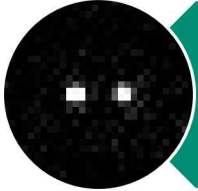




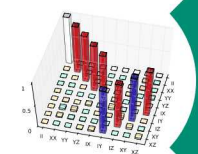
# Trap fabrication capabilities



HOA trap



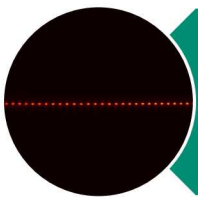
Classical control



Quantum operations



QSCOUT Quantum testbed

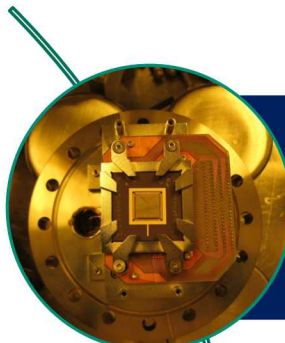
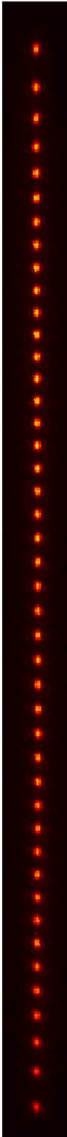


QSCOUT System engineering

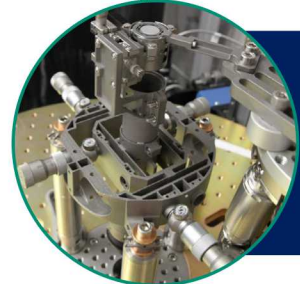


## Testbed systems designed for open access to support scientific applications

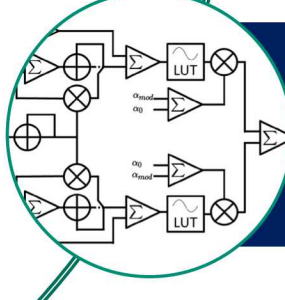
- High-fidelity operations  $\#gates \propto (\#qubits)^2$
- Gate-level access
- Open system with fully specified operations and hardware
- Low-level access for optimal control down to gate pulses
- Open for comparison and characterization of gate pulses
- Open for vertical integration by users



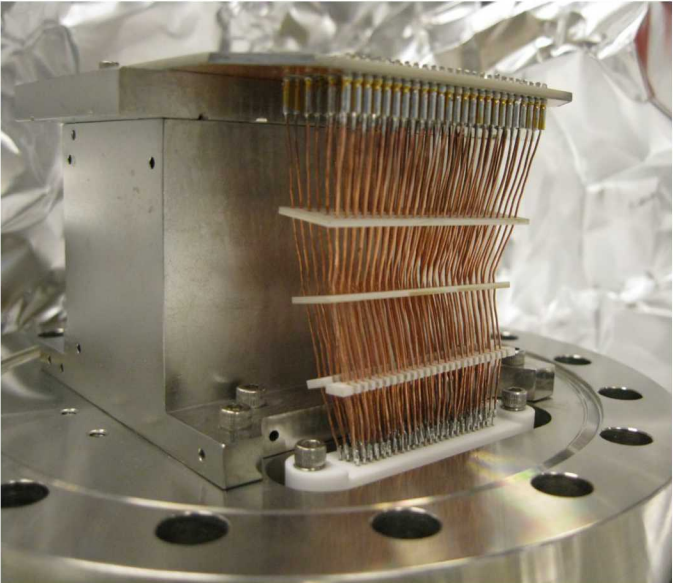
Reducing background collisions  
Vacuum technology



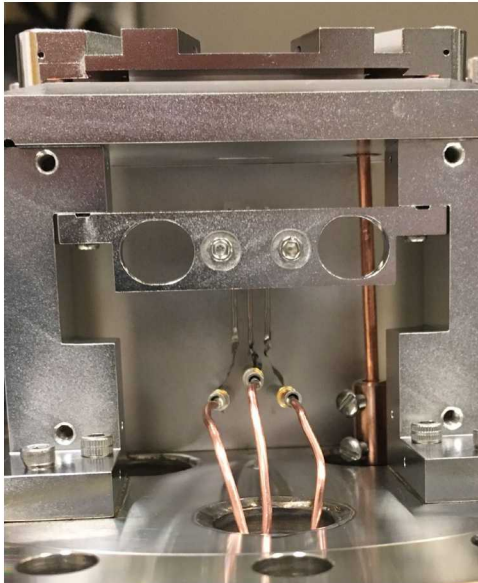
Individual addressing  
Optical and mechanical engineering



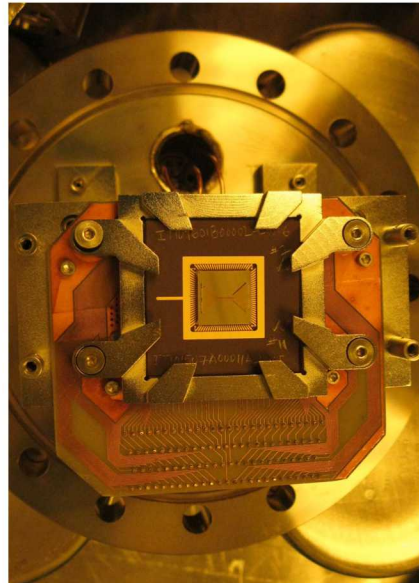
Coherent Pulse control  
Electrical engineering



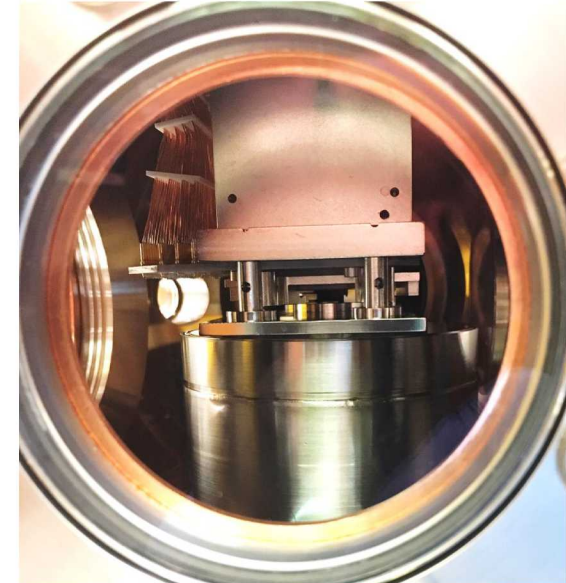
Bare copper wires with  $\text{Al}_2\text{O}_3$  spacers



3 Yb ovens (loading slot, Peregrine loading hole, HOA loading hole)



Trap installed for final bake



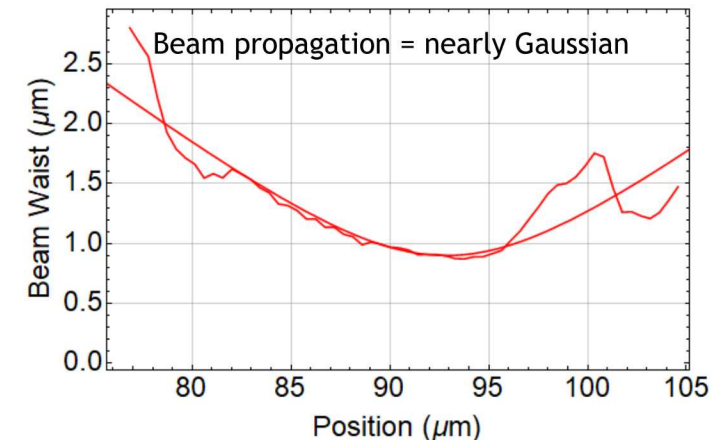
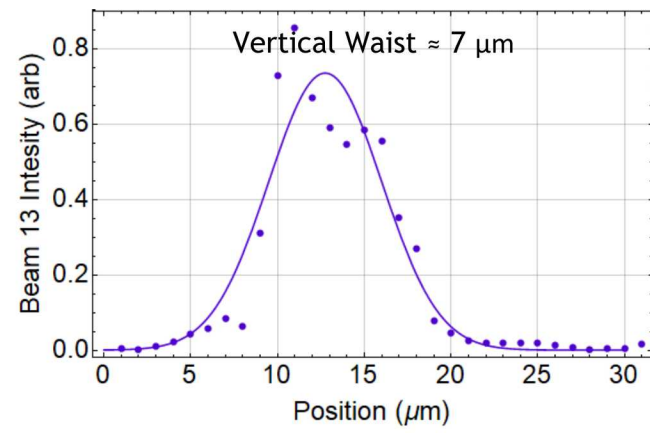
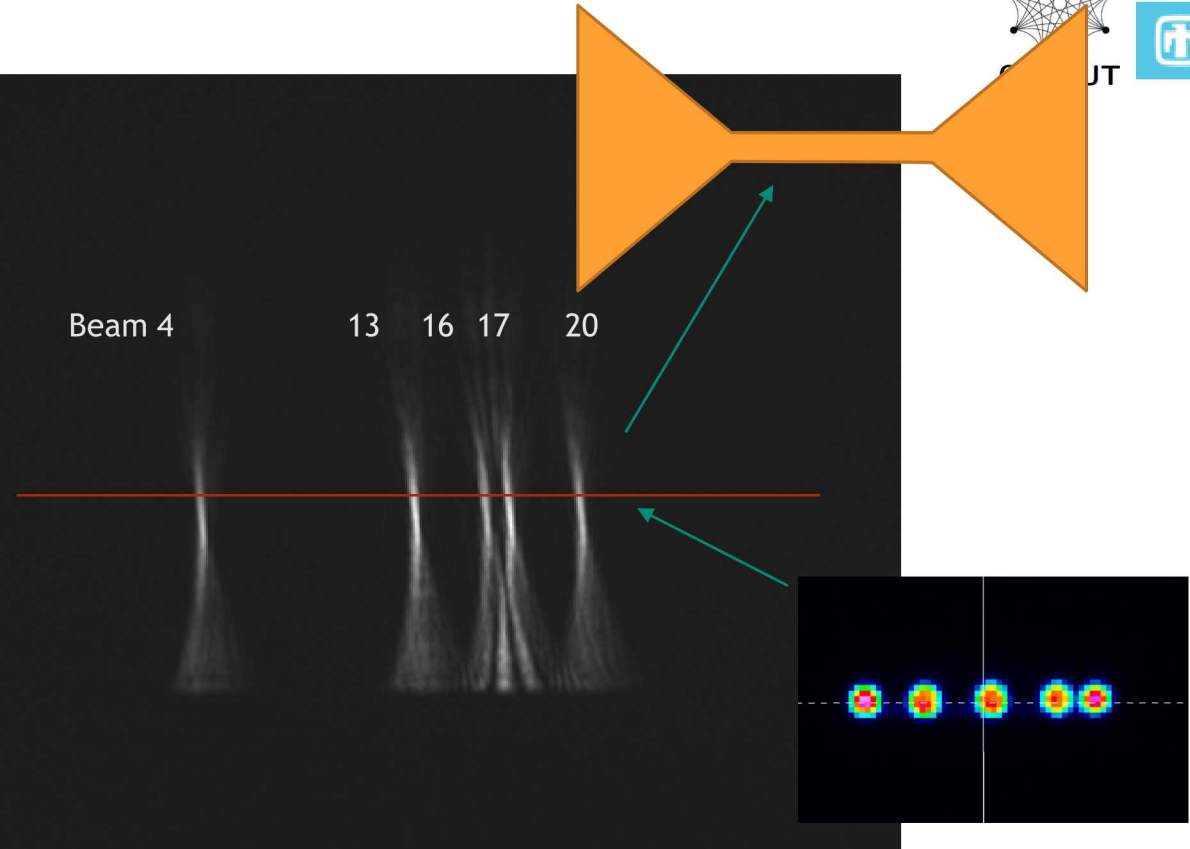
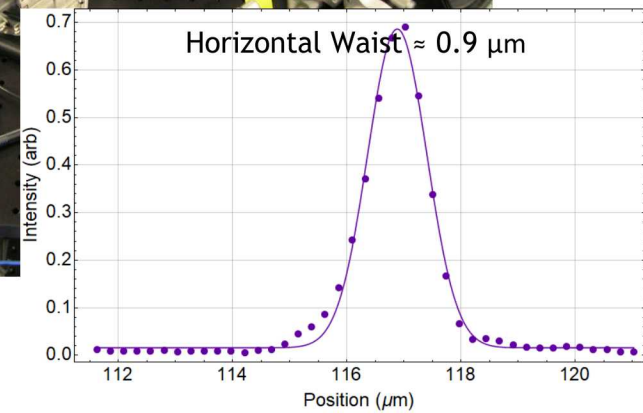
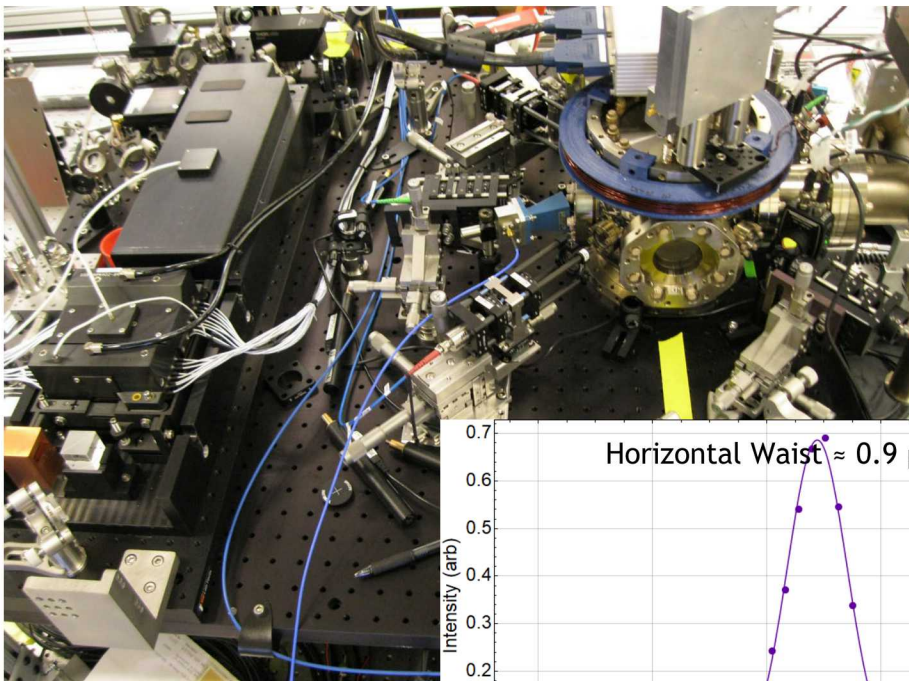
Trap platform in chamber, both re-entrants visible

### Features (hydrogen and organic mitigation):

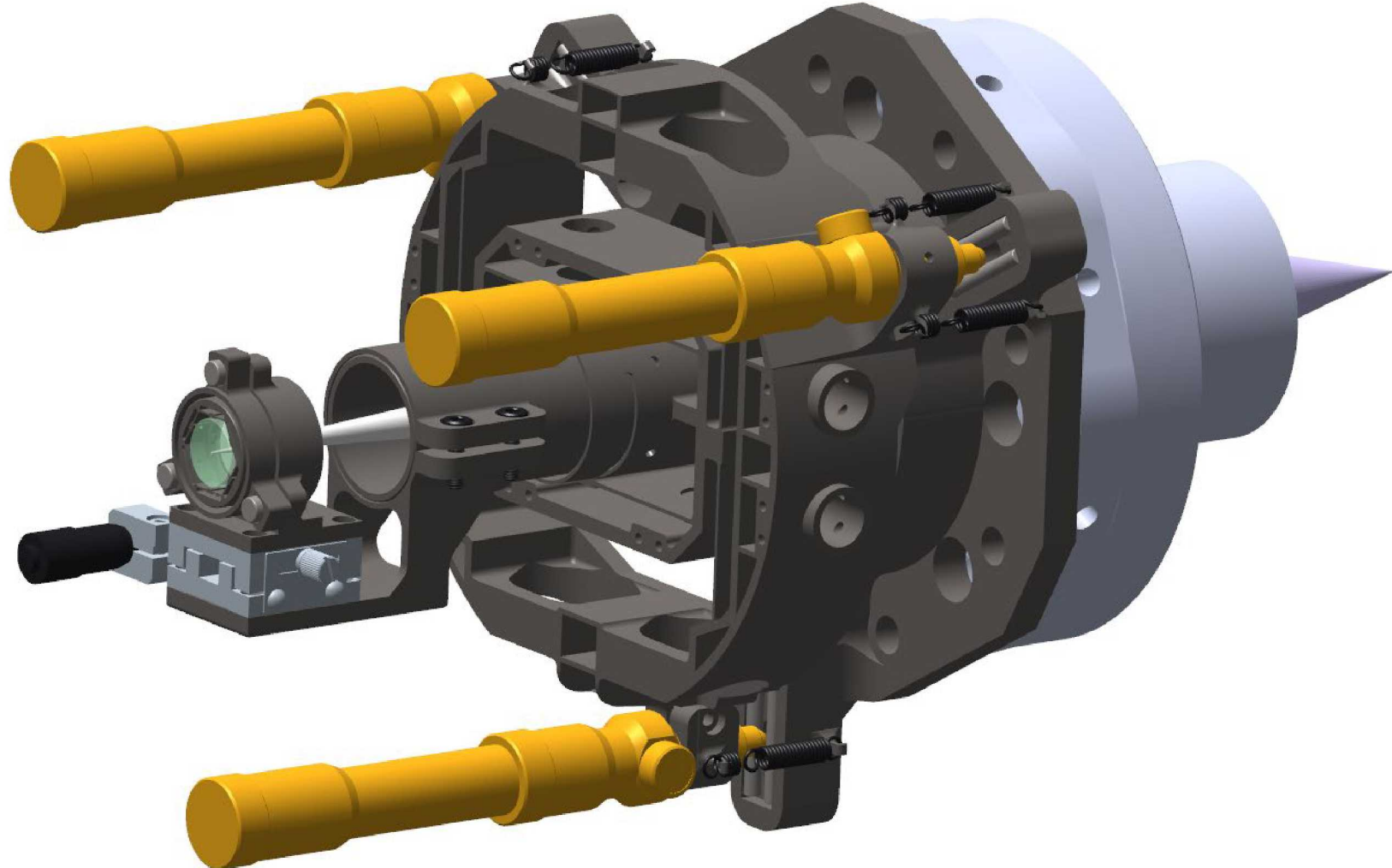
- 316L stainless steel subjected to high-temp bake process for UHV performance
- Ceramics: MACOR fuzz button spacer & Micro-D, AlN  $\rightarrow$   $\text{Al}_2\text{O}_3$  circuit board,  $\text{Al}_2\text{O}_3$  wire spacers
  - Changing circuit board to  $\text{Al}_2\text{O}_3$  allows for direct soldering of wires to board
- Bare copper wires for RF and DC voltages
- 50 L/s ion pump (previous chambers of similar form factors have used 25 L/s pumps)

## Status - Alignment Complete

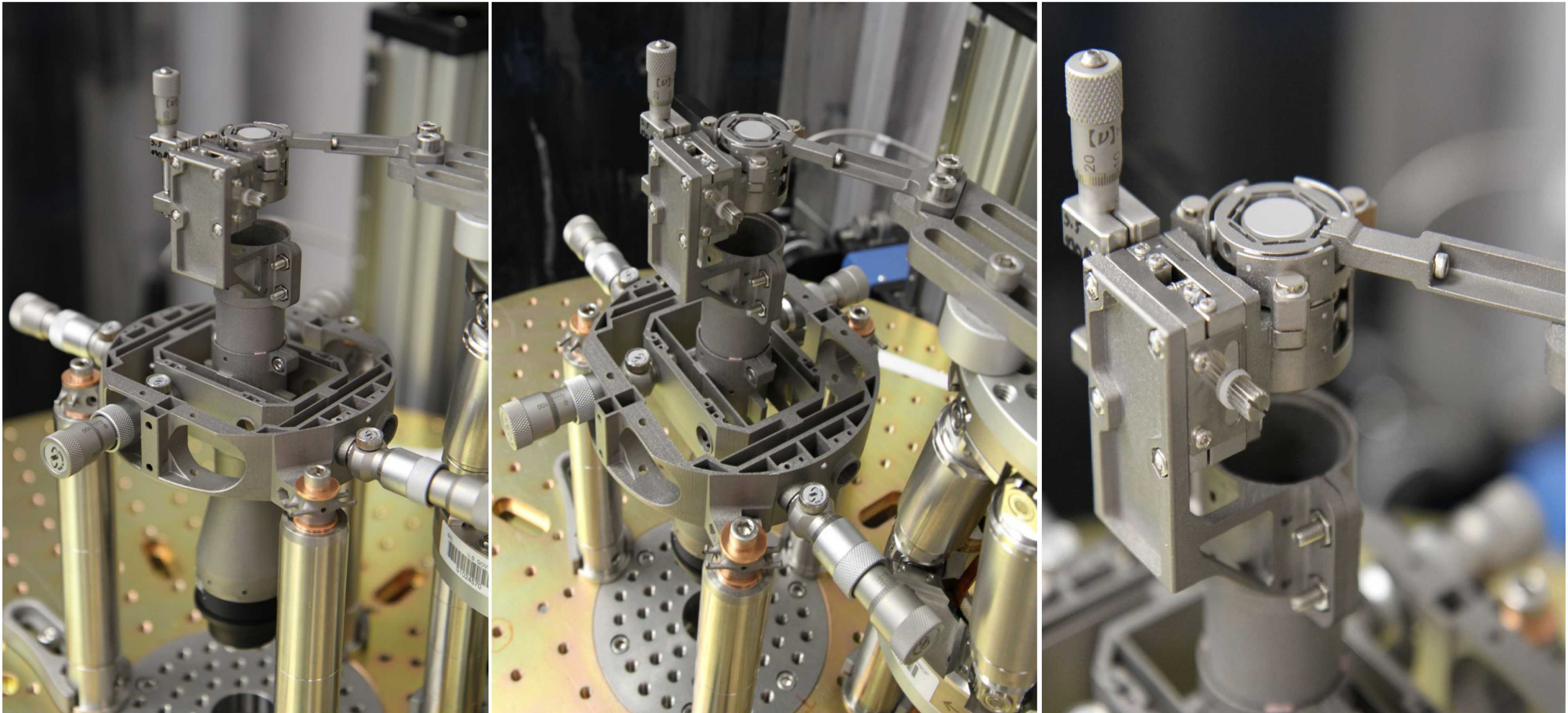
- Adjacent beams are clearly separated, and about  $5 \mu\text{m}$  apart.
- The beam waists are nearly the designed values.
- The apparent optical crosstalk is small, but we need to measure using an ion.



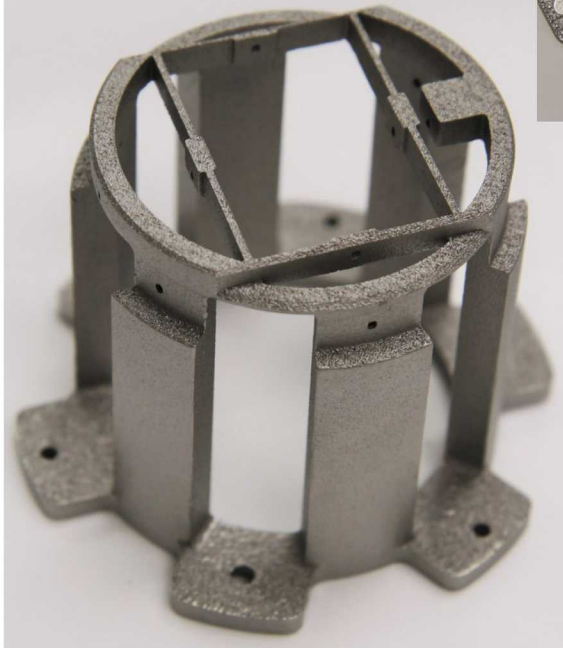
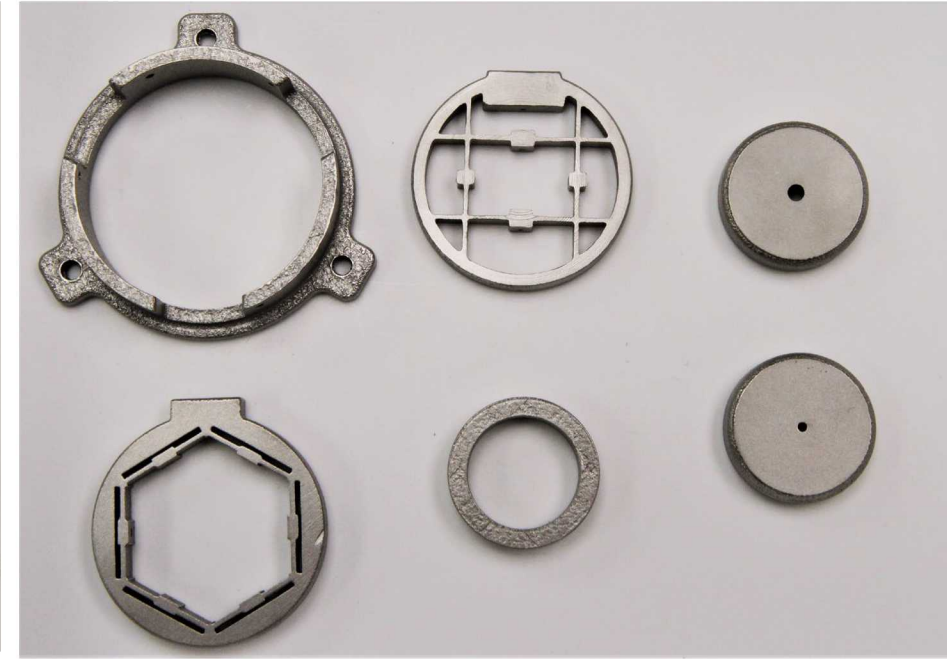
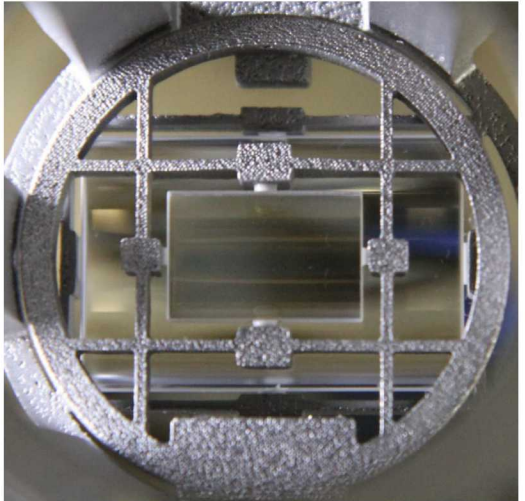
# Individual Addressing Relay Subassembly



# Individual Addressing Relay Subassembly



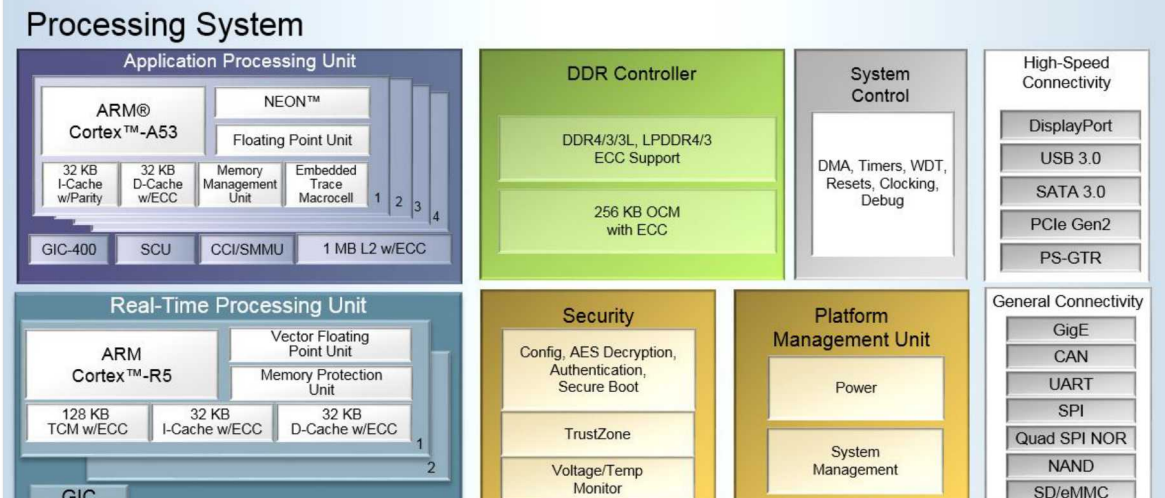
# Flexture mounts for active alignment



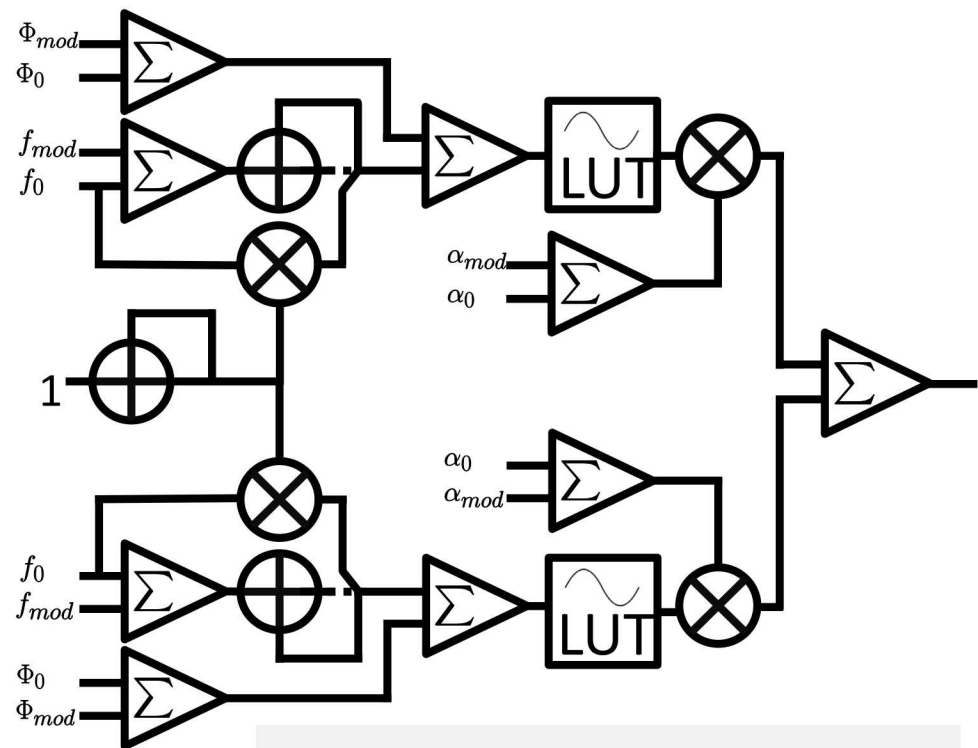
# RFSoC for coherent pulse generation

- Two tones per channel
- Coherent output synchronized between all channels
- Pulse envelopes and frequency- phase- modulation defined by splines
- Compact representation of gates for efficient streaming of circuits
- AOM Cross-talk compensation

## Radio-Frequency System on a Chip



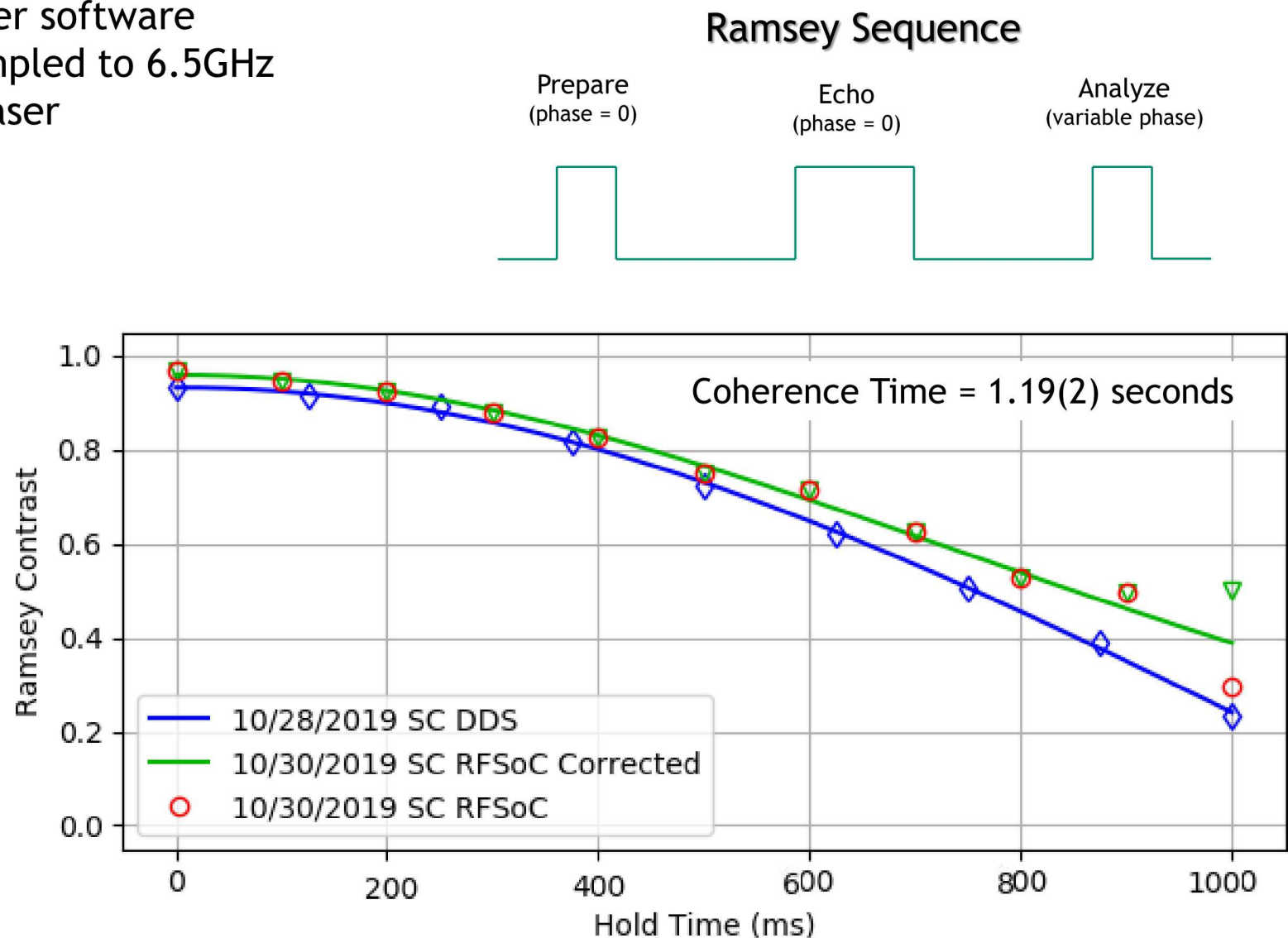
## Programmable Logic



- Completed FPGA logic design and server software
- 8 channels, 818 MHz data rate, up-sampled to 6.5GHz
- Integrated beat-note lock for pulsed laser

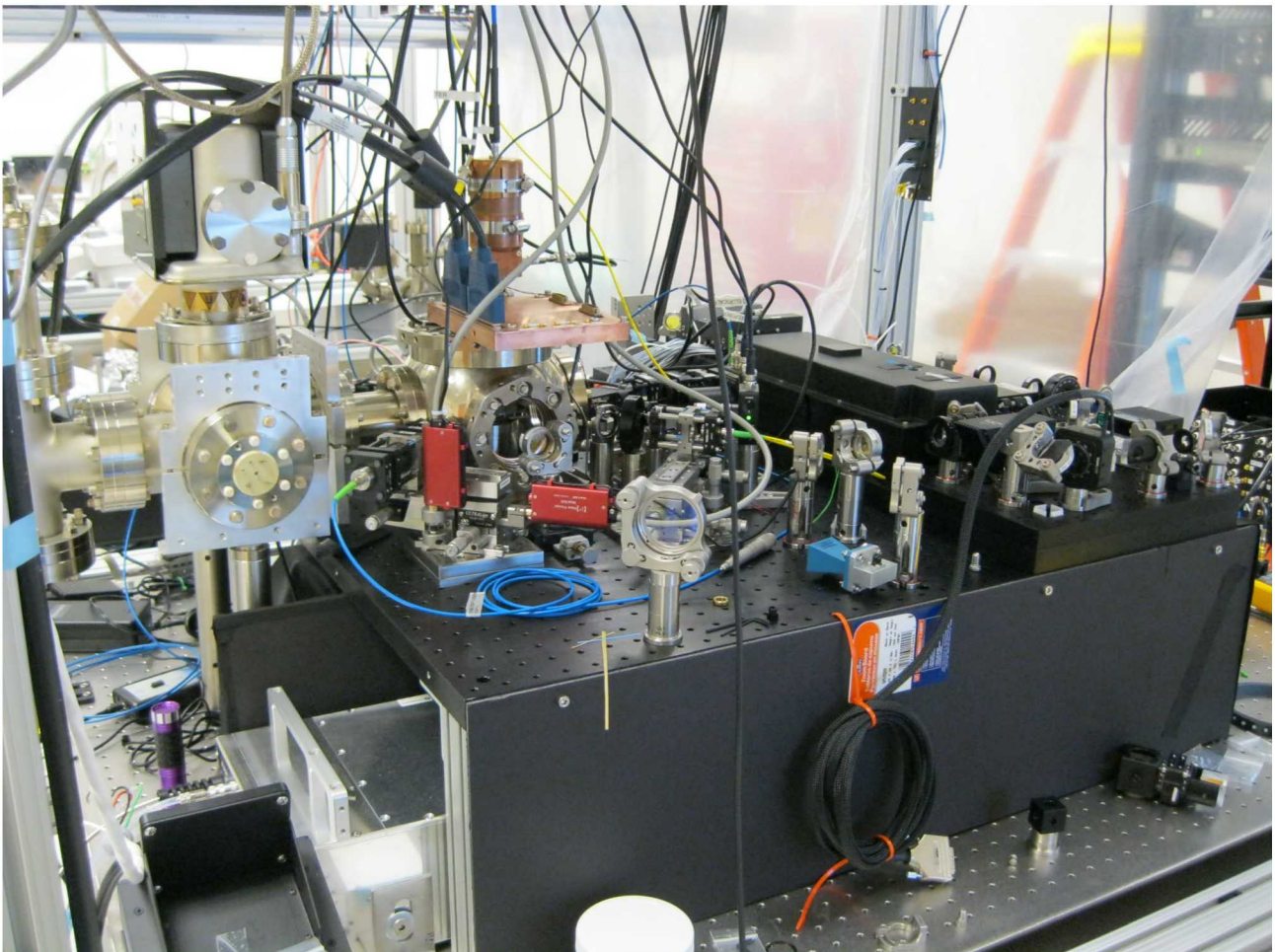
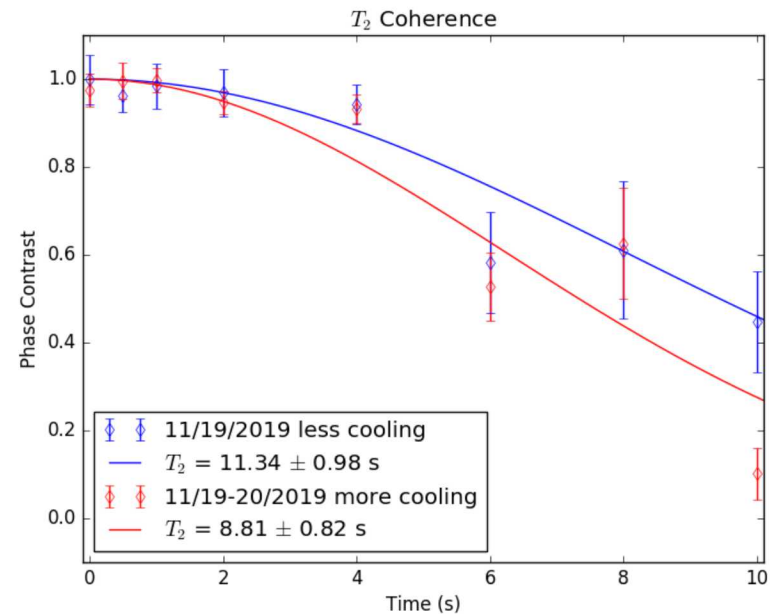
First test:

- Coherence time comparison between RFSoC system and legacy DDS based system
- Measured on legacy ion system
- Measured coherence time of 1.19s slightly better than legacy system
- Limited by experimental setup



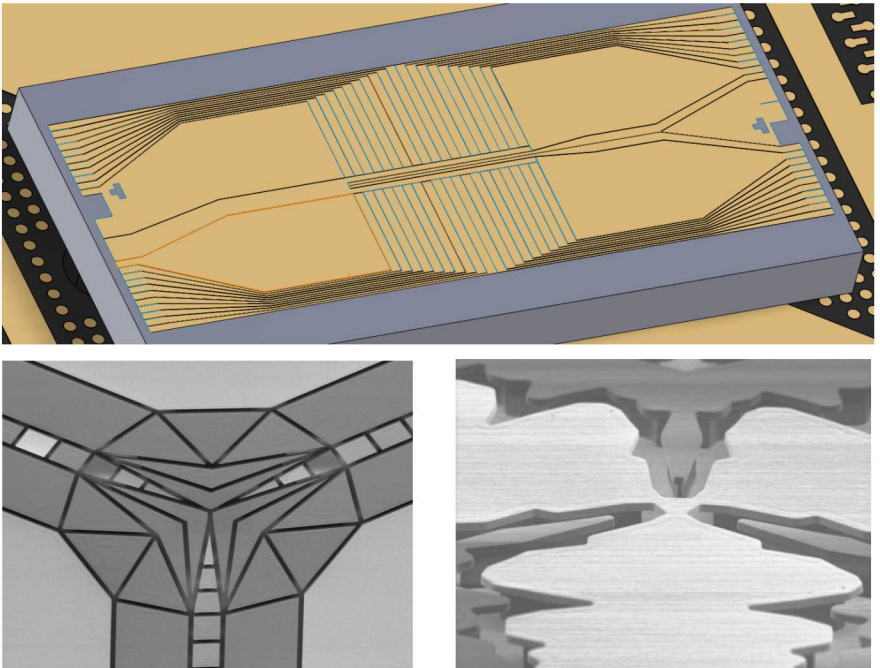
# QSCOUT system currently being assembled

- Trapped ions
- Vacuum pressure seems very promising (will measure background collisions using W-potential)
- State preparation and detection established
- Coherence time (single echo pulse)  $>8$ s



## Outlook: Trap design fabrication and integration

- Ion heating @ cryogenic temperatures
- Ion transport and quantum register reconfiguration
- Junction design and operation
- Charging of traps leading to ion shifts
- Simplification of trap fabrication
- Integration of optics and electronics



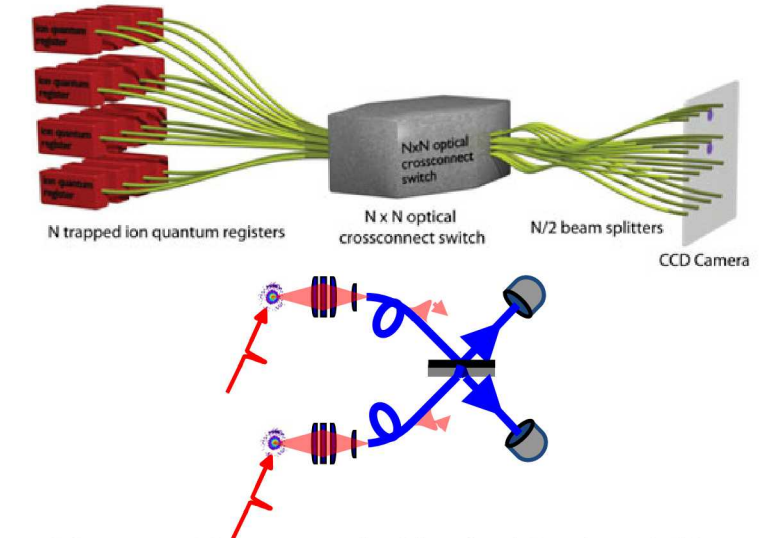
## Outlook: Scaling

- Photonic interconnect to scale beyond a single trap chip
- Integration of an optical cavity with microfabricated traps
  - For UV light, cavity finesse much lower than in infrared
  - Dielectric mirrors of cavities subject to charging
  - Possibility: Use infrared transitions to meta-stable states for entanglement and transfer quantum state to hyperfine qubit

### New gate technologies:

- Ultra-fast gates
  - Use short pulse train from pulsed laser
- Rydberg gates
  - Use Rydberg states as demonstrated in neutral atoms and recently in trapped ions

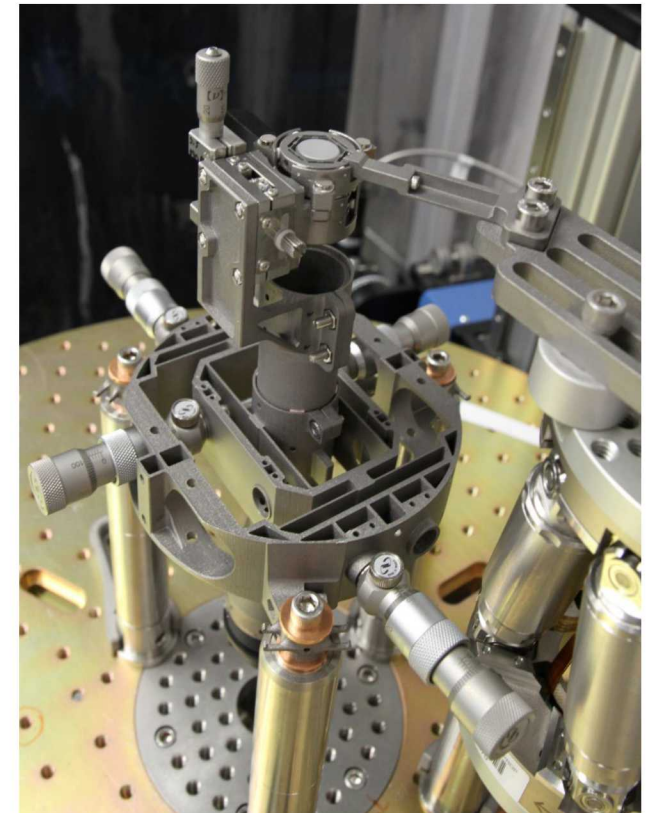
Distributed quantum networks with ions as memories



Monroe, Maunz et al., *Physical Review A* 89, 022317 (2014).

# Outlook: Systems engineering

- Vacuum Technology
- Mechanical Engineering
- Electrical Engineering





# Thanks

## *Trap design and fabrication*

Matthew Blain  
Jason Dominguez  
Ed Heller  
Corrie Herrmann  
Becky Loviza  
John Rembetski  
Paul Resnick  
SiFab team

## *Mechanical Engineering*

Jessica Pehr  
Zachary Kreiner

## *Trap packaging*

Ray Haltli  
Andrew Hollowell  
Anathea Ortega  
Tipp Jennings

## *Theory*

Setso Metodi  
Brandon Ruzic

## *Drift detection*

Tim Proctor  
Kevin Young

## *Trap design and testing*

Peter Maunz  
Craig Hogle  
Daniel Lobser  
Melissa Revelle  
Dan Stick  
Christopher Yale

## *RF Engineering*

Christopher Nordquist  
Stefan Lepkowski